



Recent Diagnostic Developments on LHD



Shigeru Sudo for LHD Diagnostics Team*
National Institute for Fusion Science
Toki, Japan

Recent Photo of NIFS site: 470,000m²

***LHD Diagnostics Team and Collaborators:**

**Y. Nagayama, B. J. Peterson, K. Kawahata, T. Akiyama, N. Ashikawa, M. Emoto,
M. Goto, Y. Hamada, K. Ida, T. Ido, H. Iguchi, S. Inagaki, M. Isobe, T. Kobuchi,
A. Komori, Y. Liang, S. Masuzaki, T. Minami, T. Morisaki, S. Morita, O. Motojima,
S. Muto, Y. Nakamura, H. Nakanishi, Y. Narushima, K. Narihara, M. Nishiura,
A. Nishizawa, S. Ohdachi, M. Osakabe, T. Ozaki, R. O. Pavlichenko, S. Sakakibara,
K. Sato, M. Shoji, N. Tamura, K. Tanaka, K. Toi, T. Tokuzawa, K. Y. Watanabe,
T. Watanabe, H. Yamada, I. Yamada, M. Yoshinuma, P. Goncharov¹, D. Kalinina¹,
T. Sugimoto¹, T. Kanaba¹, A. Ejiri², Y. Ono², S. Kado², H. Hojo³, K. Ishii³, N. Iwama⁴,
Y. Kogi⁵, A. Mase⁵, M. Sakamoto⁵, K. Kondo⁶, H. Nagasaki⁶, S. Yamamoto⁶, N. Nishino⁷,
S. Okajima⁸, T. Saida⁹, M. Sasao⁹, T. Takeda¹⁰, S. Tsuji-lio¹¹, D. S. Darrow¹²,
H. Takahashi¹², Y. Liu¹³, J.F. Lyon¹⁴, A. Yu. Kostrioukov¹⁵, V. B. Kuteev¹⁵, V. Sergeev¹⁵,
I. Viniar¹⁵, A. V. Krasilnikov¹⁶, A. Sanin¹⁷, L. N. Vyacheslavov¹⁷, D. Stutman¹⁸,
M. Finkenthal¹⁸ and LHD Team**

National Institute for Fusion Science, Toki, Japan

¹*Graduate University for Advanced Studies, Hayama, Japan*

²*University of Tokyo, Tokyo, Japan*

⁴*Daido Institute of Technology, Nagoya, Japan*

⁶*Kyoto University, Uji, Japan*

⁸*Chubu University, Kasugai, Japan*

¹⁰*Univ. of Electro-Communications, Chofu, Japan* ¹¹*Tokyo Institute of Technology, Tokyo, Japan*

¹²*Princeton Plasma Physics Laboratory, Princeton, New Jersey, USA*

¹³*South Western Institute of Physics, Chengdu, China*

¹⁴*Oak Ridge National Laboratory, Oak Ridge, Tennessee, USA*

¹⁵*St. Petersburg Technical University, St. Petersburg, Russia*

¹⁶*Troitsk Institute for Innovating and Fusion Research, TRINITI, Troitsk, Russia*

¹⁷*Budker Institute of Nuclear Physics, Novosibirsk, Russia*

¹⁸*Johns Hopkins University, Baltimore, Maryland, USA*

* Transport and Core Plasma Property

P-3.18 **Structures on Electron Temperature Profiles of the Plasmas Confined in the Large Helical Device** by K.Narihara et al.

P-3.19 **Influence of Beam Flow on the Electron Transport in Low Density LHD Discharges** by N.Ohyabu.

P-3.16 **Global and Local Confinement Scaling Laws of NBI-Heated Gas-puffing Plasmas on LHD** by K.Yamazaki et al.

P-2.160 **Effect of Magnetic Field on Asymmetric Radiative Collapse in the Large Helical Device** by N. Ashikawa et al.

P-4.67 **Imaging Bolometer for a Burning Plasma Experiment** by B.J. Peterson et al.

* Turbulence & Fluctuations

P-1.73 **Imaging Interferometer for Plasma Density Profile and Microturbulence Study on LHD** by A.L.Sanin et al.

P-3.11 **Particle transports and related fluctuation on LHD** by K.Tanaka et al.

P-3.174 **Edge Plasma Turbulence in Fusion Devices: Bursty Behavior and Fractal Properties** by V.P. Budaev et al.

* MHD

O-3.2A(P-2.230) **Effect of L-H Transition on MHD Stability near the Plasma Edge in the Large Helical Device** by K.Toi et al.

P-3.21 **Sawtooth Oscillation in Current Carrying Helical Plasma in LHD** by Y.Nagayama et al.

P-3.17 Interpretation of Low-Frequency and High-Frequency Alfvén Instabilities in NBI Experiments on LHD by Y.I. Kolesnichenko et al.

*Heating

P-2.171 Achievement of a High Ion Temperature with Ne- and Ar-Seeded Discharges by High-Power NBI Heating in LHD by Y.Takeiri et al.

P-2.181 Analysis of ICRF Heating in LHD by Three-Dimensional Calculation by T.Seki et al.

* Fueling and Pellet

P-1.59 Fast spectroscopic measurements of the ablation clouds of Tracer-Encapsulated Solid Pellets injected into LHD plasmas by N.Tamura et al.

P-3.12 Repetitive Pellet Fueling on LHD by R.Sakamoto et al.

P-3.13 Observation of Plasma Response and Ion Temperature Increase after Impurity Pellet Injection in LHD by S.Morita et al.

P-3.14 Dynamics of pellet ablation cloud observed by a fast-framing tangentially viewing soft X-ray camera in LHD by S.Ohdachi et al.

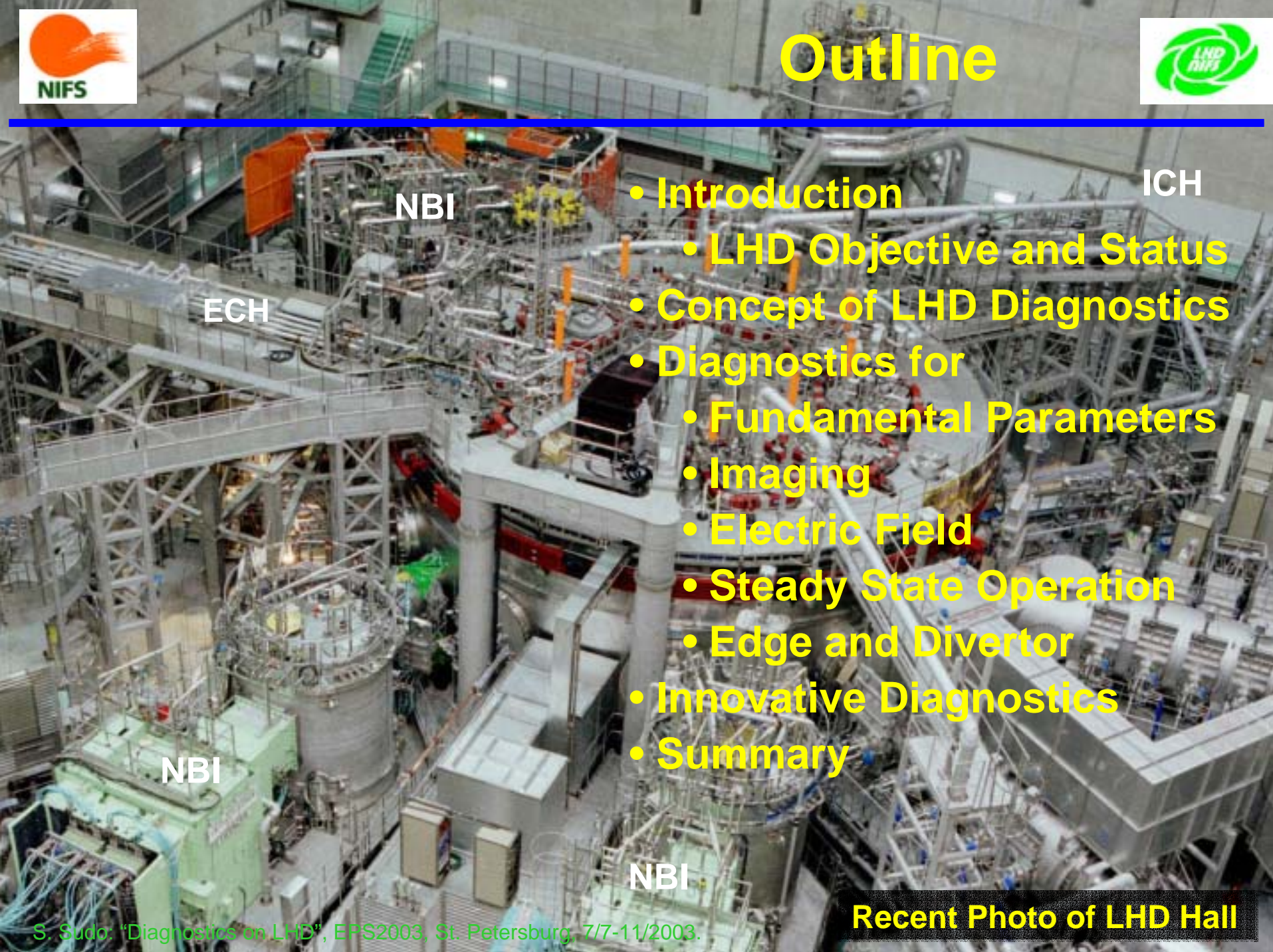
* Edge and Divertor Plasma

P-3.20 Edge Density Profile Measurements on LHD with a Lithium Beam Probe by T.Morisaki et al.

* High Energy Particles

P-3.22 Horizontal and Vertical Distributions of High-Energy Particle on Large Helical Device by T.Ozaki et al.

P-3.23 Suprathermal Proton Distribution Function Measurements with a Multidirectional Charge Exchange Diagnostic on LHD by P.R.Goncharov et al.



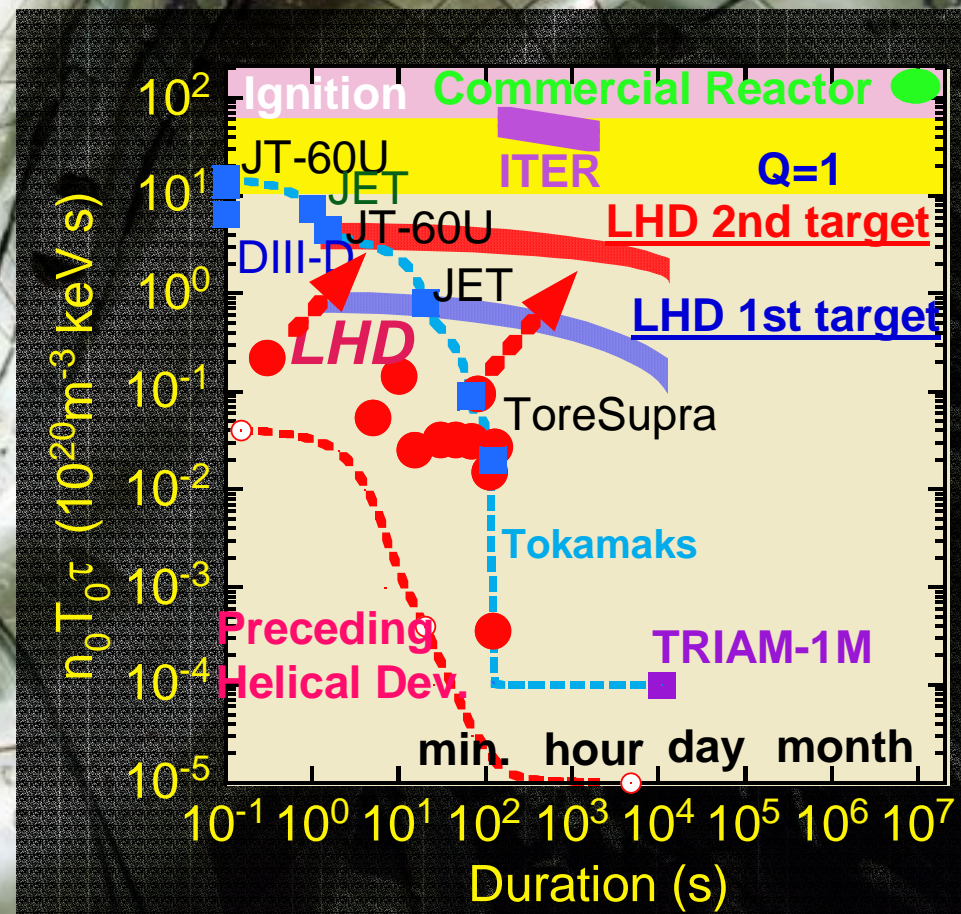
- **Introduction**
 - LHD Objective and Status
- Concept of LHD Diagnostics
- Diagnostics for
 - Fundamental Parameters
 - Imaging
 - Electric Field
 - Steady State Operation
 - Edge and Divertor
- Innovative Diagnostics
- Summary

Objective of Large Helical Device

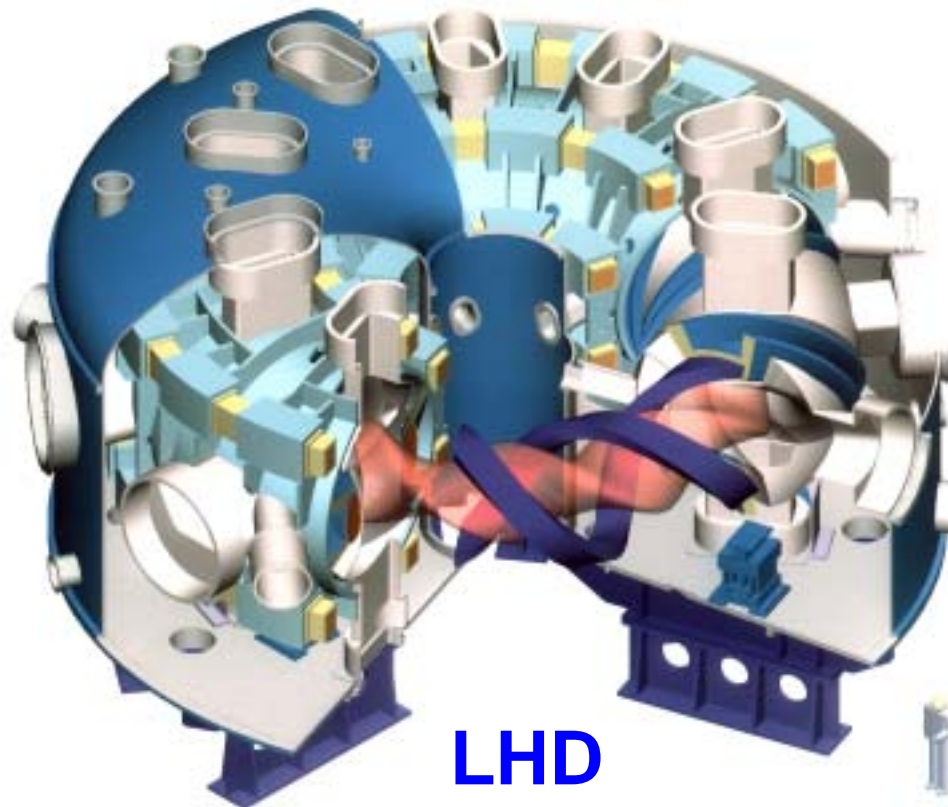
- Objective of LHD is to clarify physics of fusion relevant plasma in steady state.
- For this purpose, we are developing: Superconducting magnet, High power heating, Divertor, and Appropriate Diagnostics.



The LHD experiment started in the end of March 1998, and 6 experimental campaigns have been carried out since then.

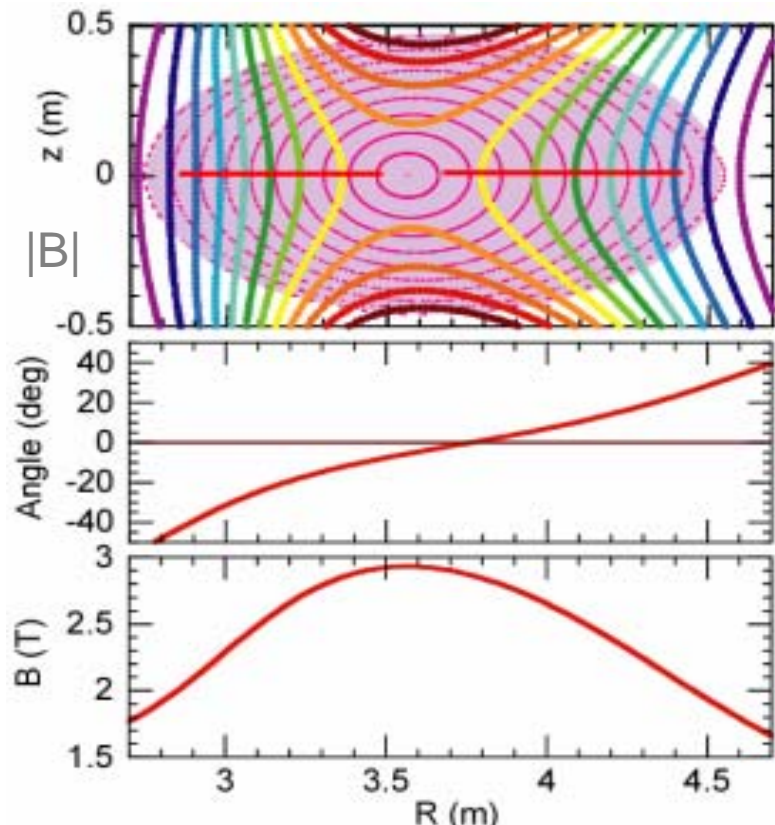


Large Helical Device (LHD)



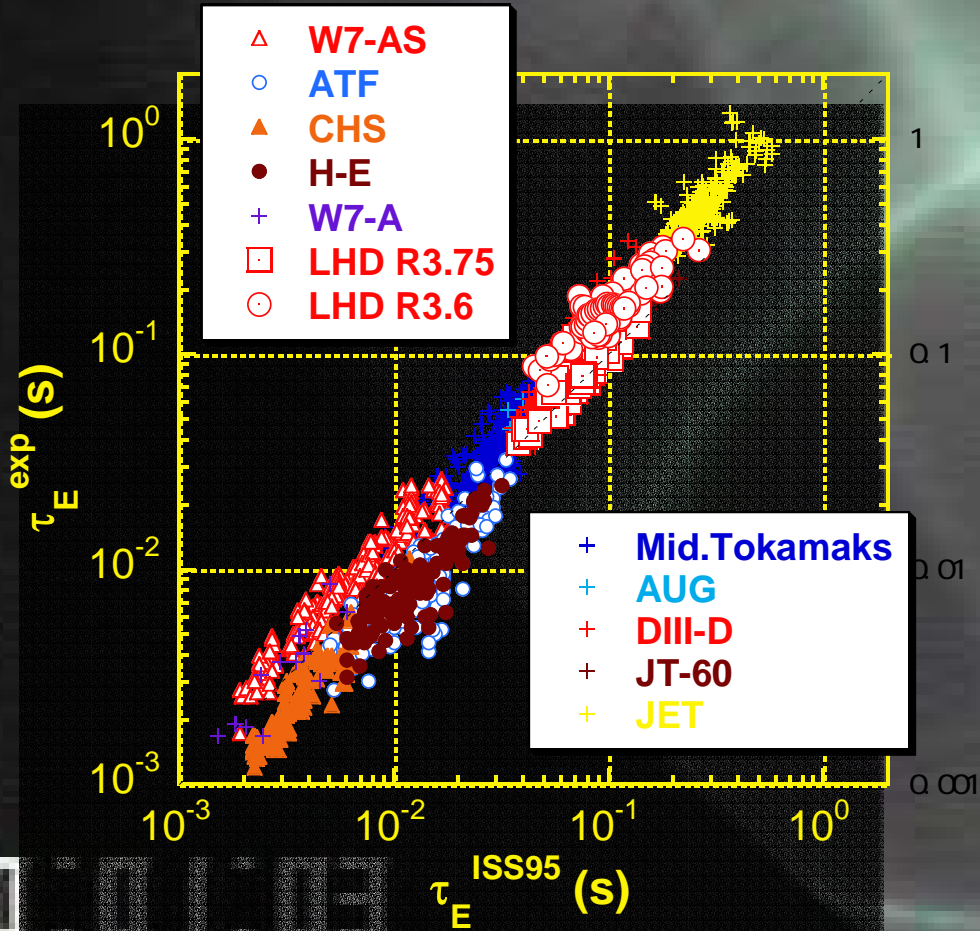
All Helical and Poloidal Coils
are superconducting.

- Heliotron configuration with $I=2/m=10$ field period
- Major radius = 3.42 - 4.1 m
Plasma radius = 0.6 m
Plasma volume = 30 m³
Toroidal field = 2.9 T



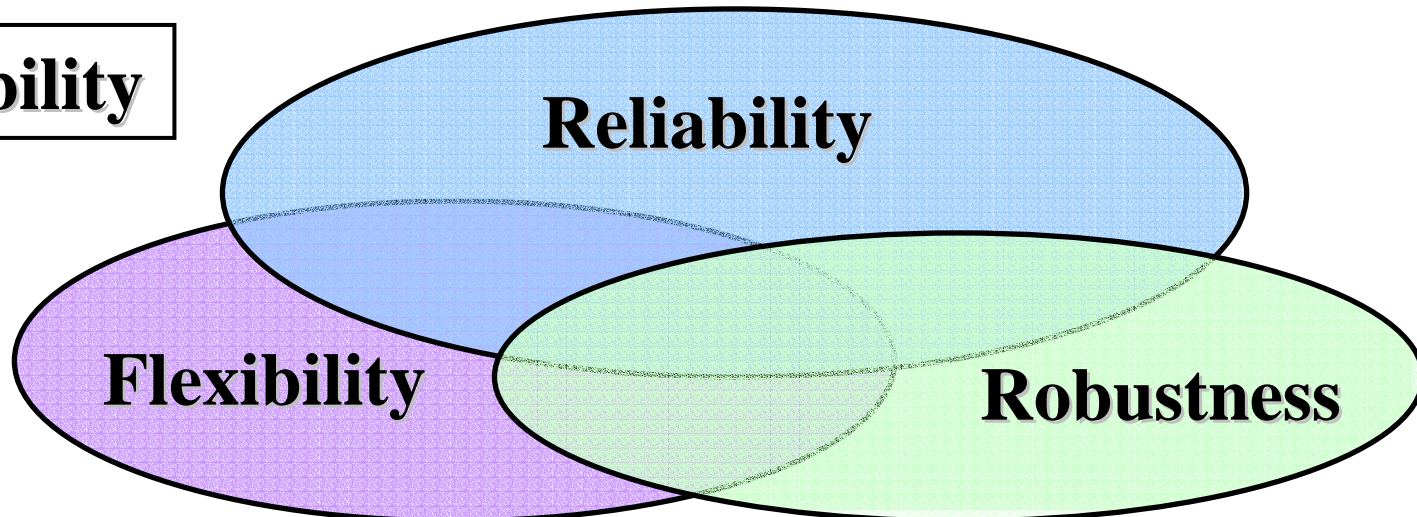
12.14

- LHD has better confinement than ISS95 scaling.
- Target temperatures have been achieved.
- High β and long pulse are next targets.

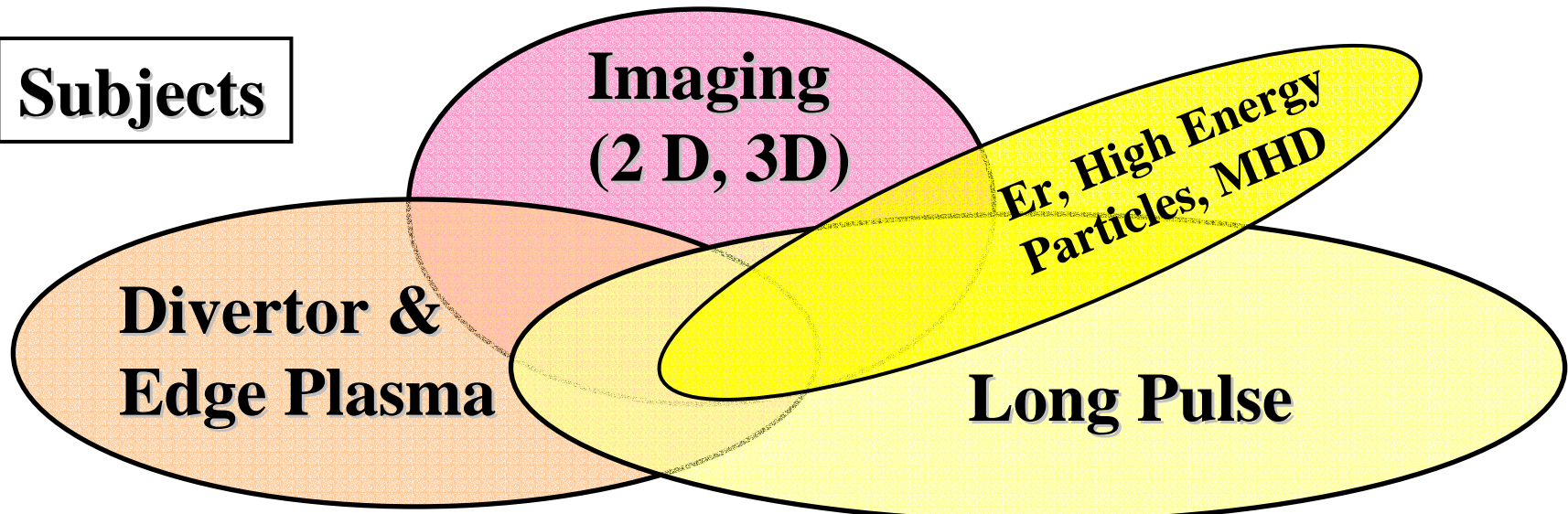


	Target	Achieved
Te	10 keV	10 keV
Ti	7 keV	7 keV
W_p	3 MJ	1.2 MJ
Beta	5 %	3.2 %
Duration	3600 s	150 s
NBI	17 MW	10.3 MW
ECH	3 MW	2.1 MW
ICH	5 MW	2.7 MW

Ability

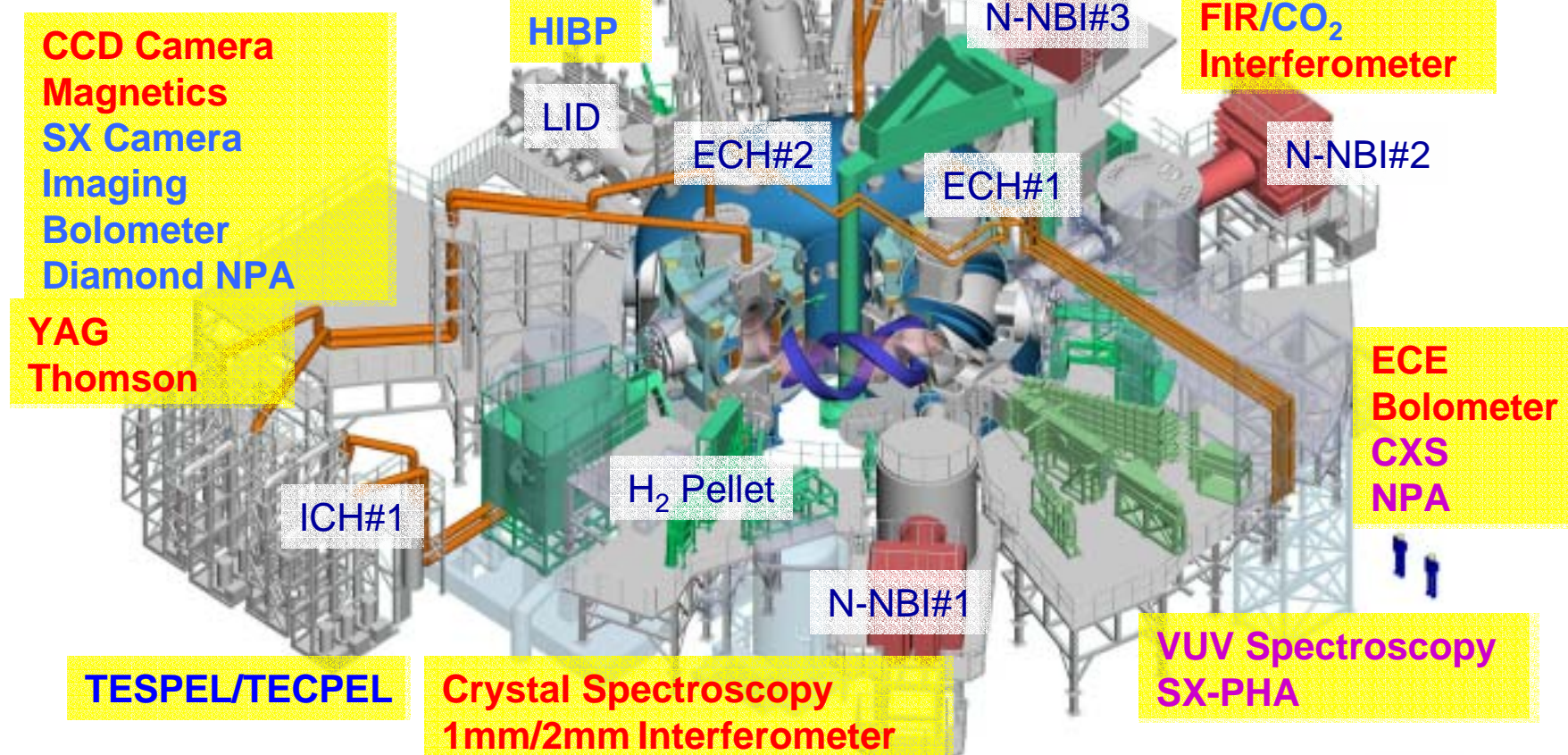


Subjects



Overview of LHD Diagnostics

- Complete set of standard diagnostics for **operation** and **physics study** have been installed.
- Advanced diagnostics are being developed with collaboration.



1. Reliable diagnostics for operation (TV, n_e , I_p , W_p , NBI interlock) and for fundamental plasma parameters (T_e , T_i , n_e).

- **Plasma Operation (Feedback Control)**

- n_e : FIR Laser Interferometer
 - **NBI Interlock: Reflectometer**
 - I_p : Rogowskii Coil

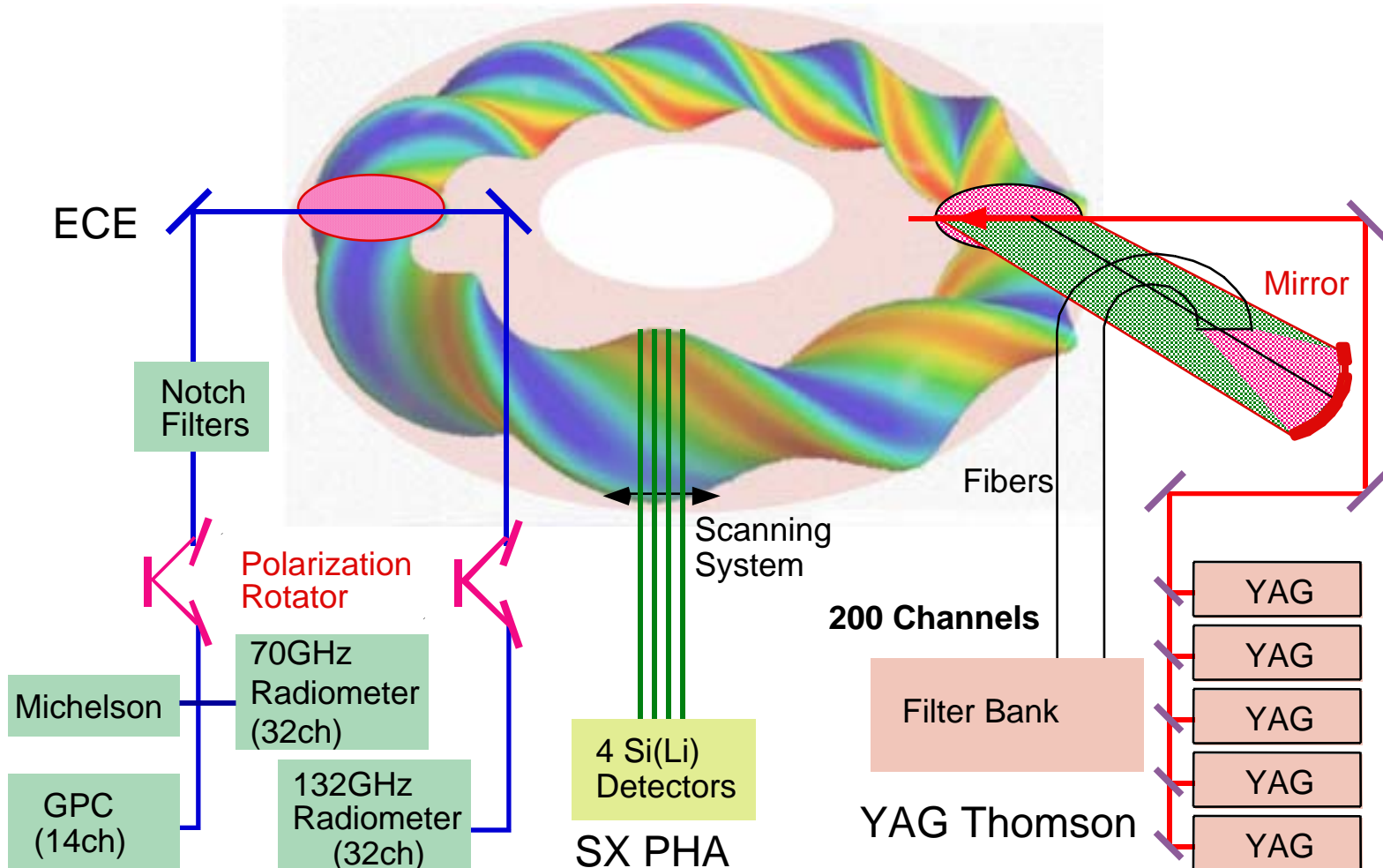
(Unlike tokamaks, in LHD, plasma current is not needed. But, the bootstrap current and beam driven current appear to some extent.)

- **Fundamental Plasma Diagnostics with Reliability and Flexibility**

- T_e : YAG Thomson, ECE (Michelson), SX-PHA
 - T_i : Crystal Spectroscopy, CXS, TOF-NPA
 - n_e : Interferometers (1&2mm micro wave, FIR, CO_2+YAG Laser)
 - W_p , β : Diamagnetic Flux Loop
 - **Data Acquisition: CAMAC, Object Oriented Database**

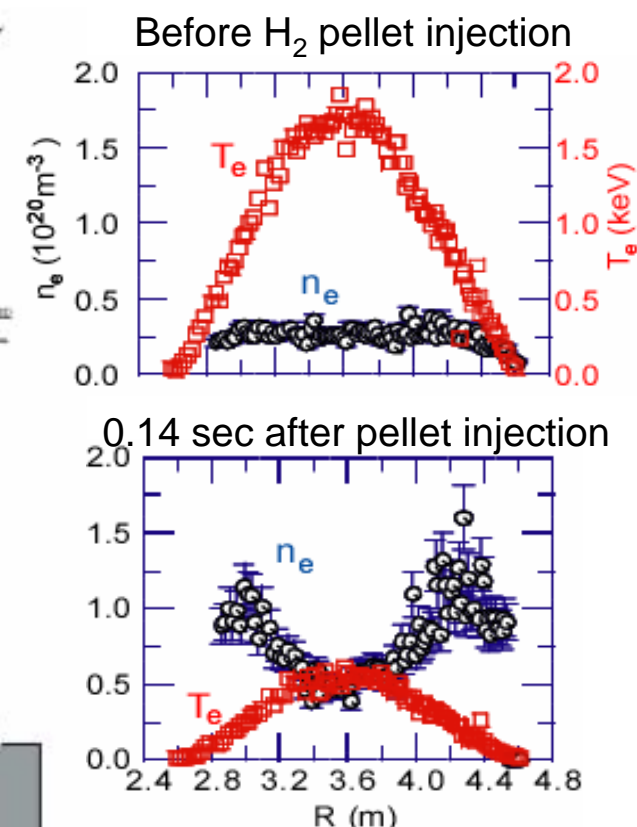
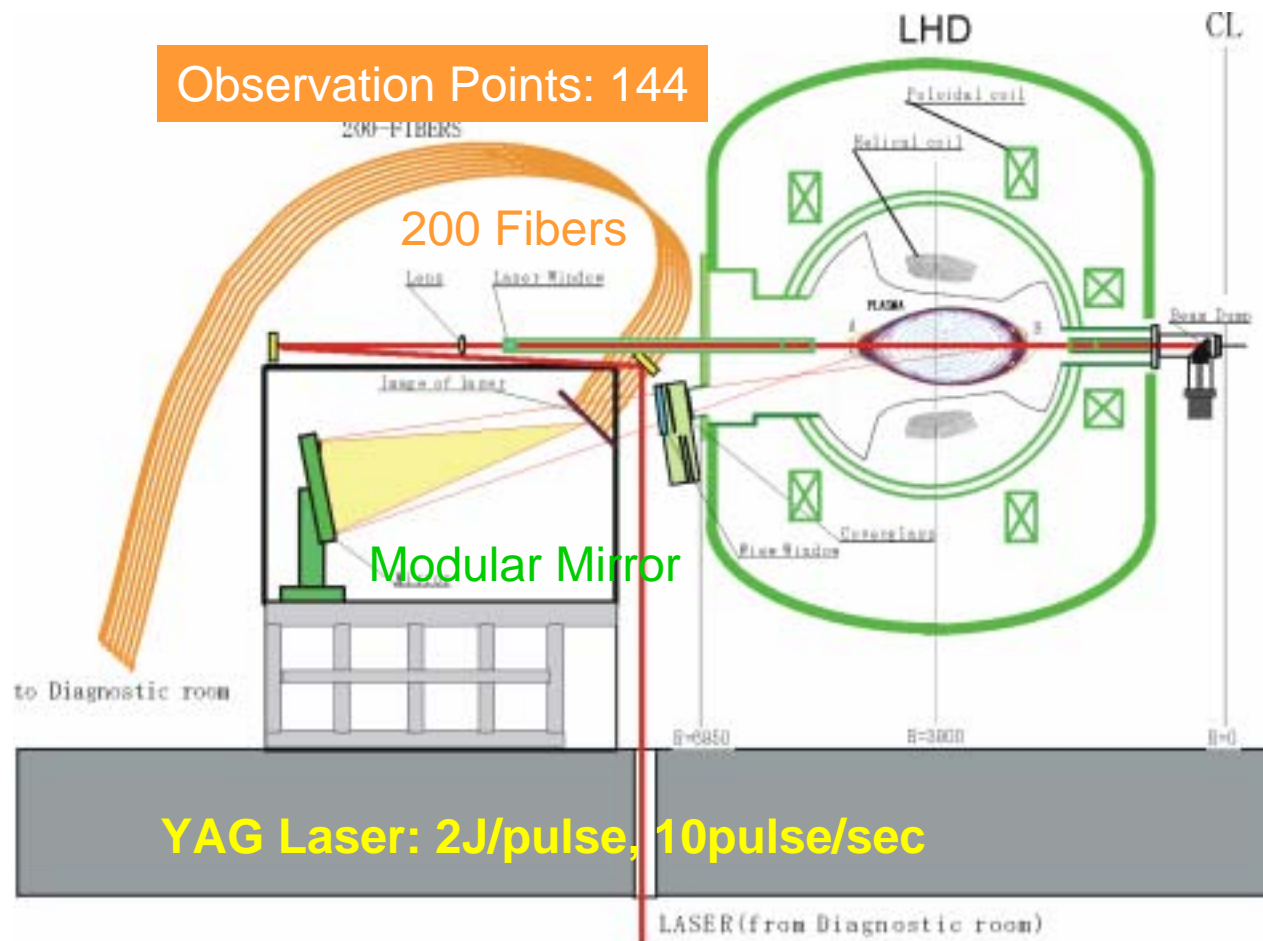
Electron Temperature Diagnostics

- Time evolution of T_e profile is measured with 3 systems.
- ECE is useful also for MHD diagnostics.
- SX-PHA is useful also for impurity measurement.



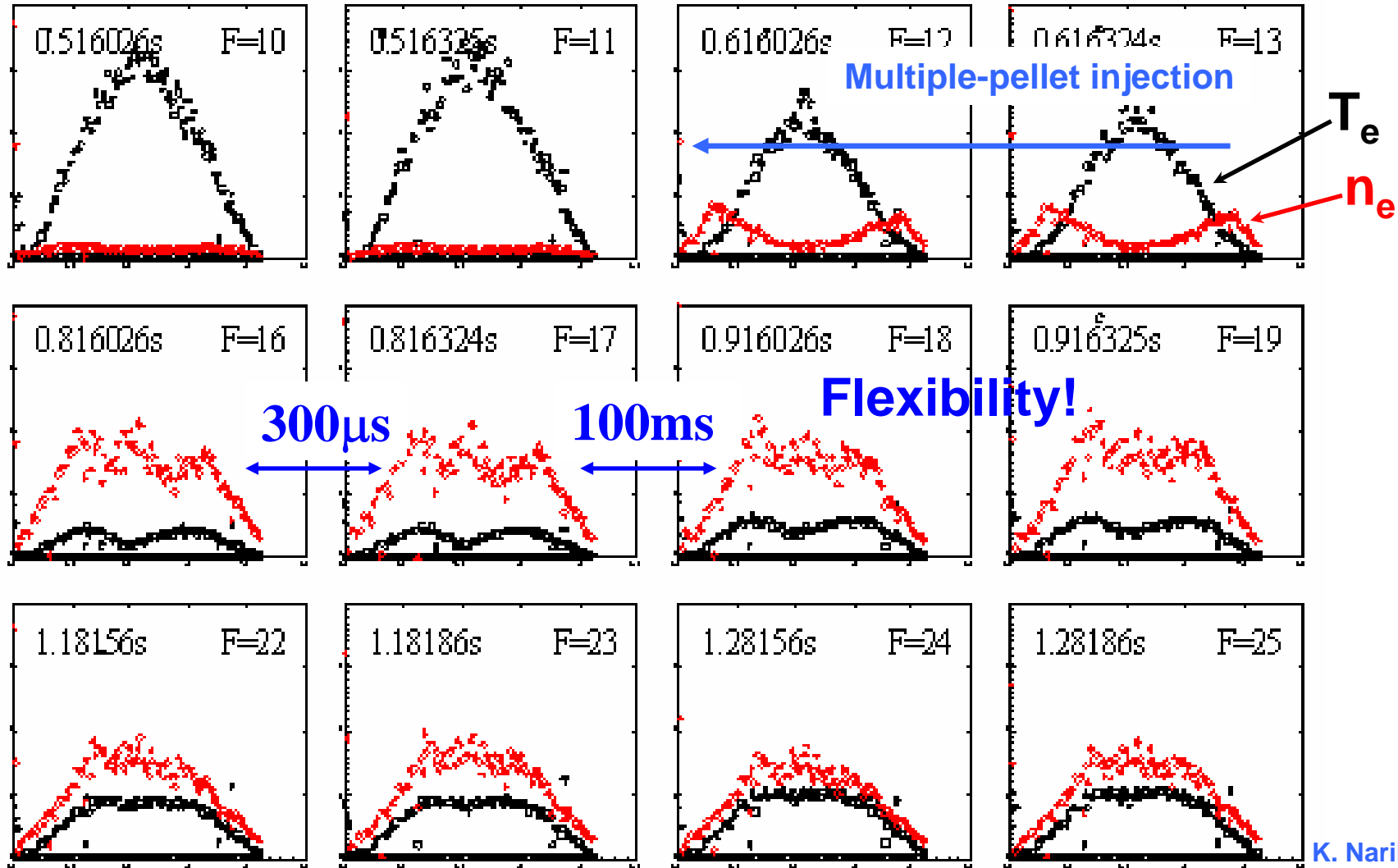
YAG Laser Thomson Scattering

- LHD Thomson uses an obliquely back-scattering configuration.
- Large mirror made of 100 modules condenses scattered light ($\Delta\Omega > 10\text{msr}$).
- 144 radial points are measured every 0.1-0.01 sec ($15\text{mm} < \Delta x < 30\text{mm}$).
- YAG Thomson system works routinely with little trouble in LHD.



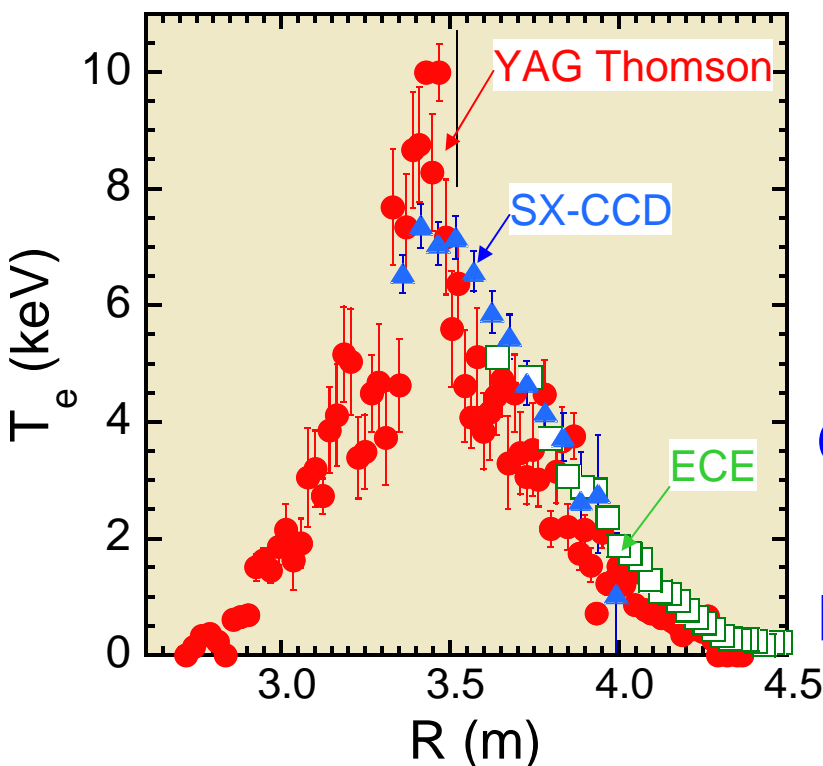
T_e and n_e profiles by YAG Thomson

#33621 B= 2.8 T

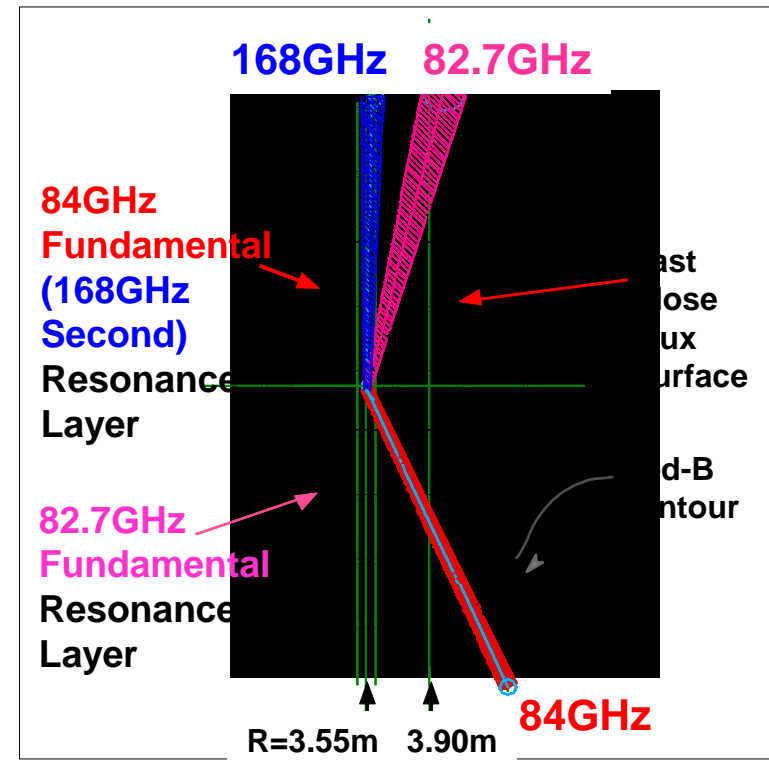


T_e by Thomson, ECE and SX

- By focusing ECH at the plasma center, high T_e plasma is obtained.
- T_e measured with Thomson, ECE and SX are consistent.
- High T_e plasma is accompanied with ITB in LHD.

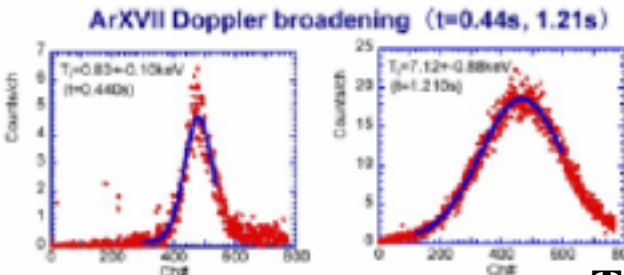


Cross check
↓
Reliability!



$B=2.9\text{T}$
 $\text{ECH}=1.2\text{MW}$
 $T_{e0}=10\text{keV}$
 $T_{i0}=2\text{keV}$
 $n_e=0.5 \times 10^{19}\text{m}^{-3}$
 $\tau_E=50\text{ms}$

Ion Temperature Diagnostics

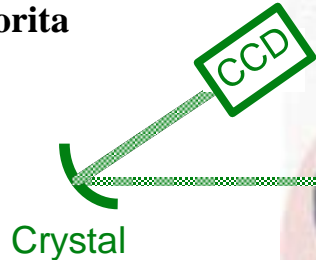


- Central ion temperature is measured by the crystal spectrometer.
- Profiles of T_i and the electric field are measured with CXS.
- T_i and fast ion spectra are measured with NPA.

$T_i(0) = 7 \text{ keV}$

Crystal Spectroscopy

S. Morita



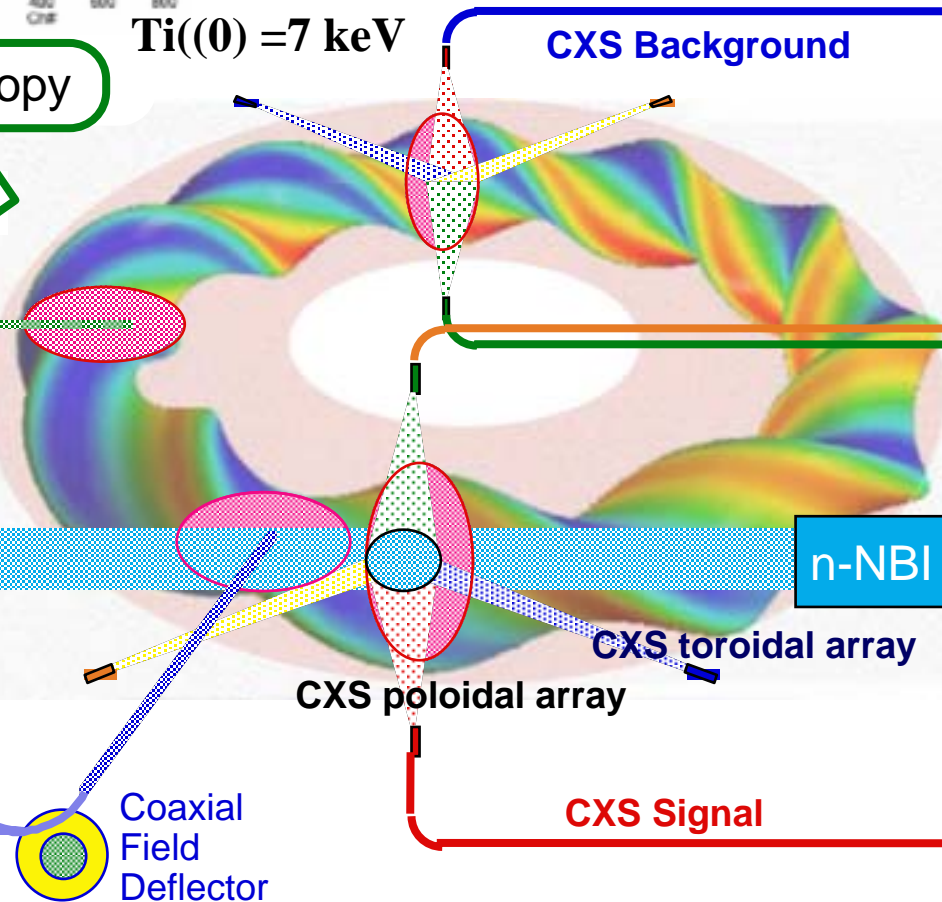
Fast Particles

T. Ozaki,
P. Goncharov,
J. Lyon

n-NBI

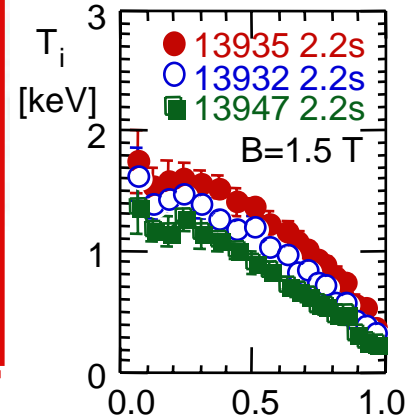
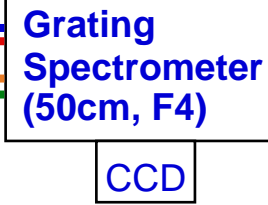
TOF tubes

NPA



K. Ida

CXS

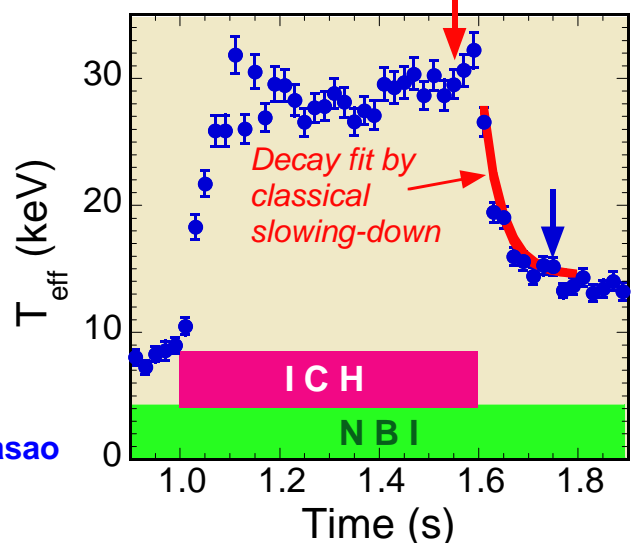
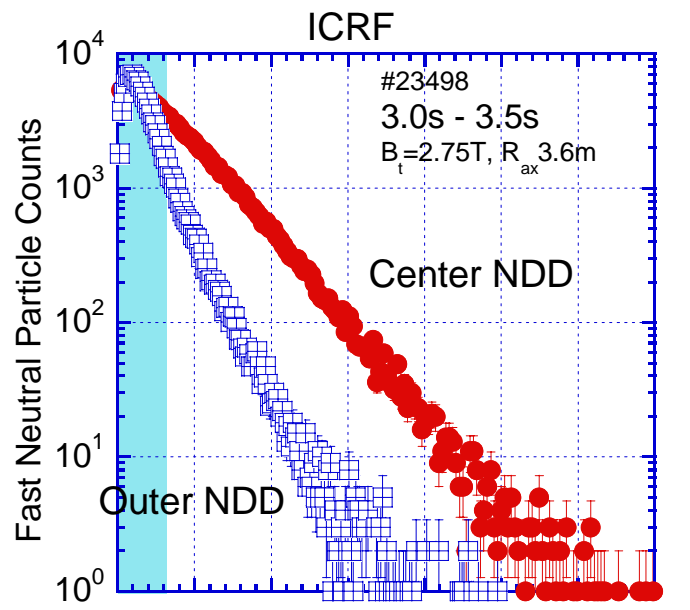


Diagnostics of Fast Particles

- Fast neutral particles escaped from LHD plasma are detected by
 - Time Of Flight Neutral Particle Analyzer
 - Natural Diamond Detectors
 - Silicon Diode Neutral Particle Analyzer
- TOF-NPA is useful for detecting low energy particles.
- NDD and SD-NPA are compact and are useful for detecting high energy particle.
- NDD measurements reveal that ICH generates fast ions and confinement of fast ions is classical.

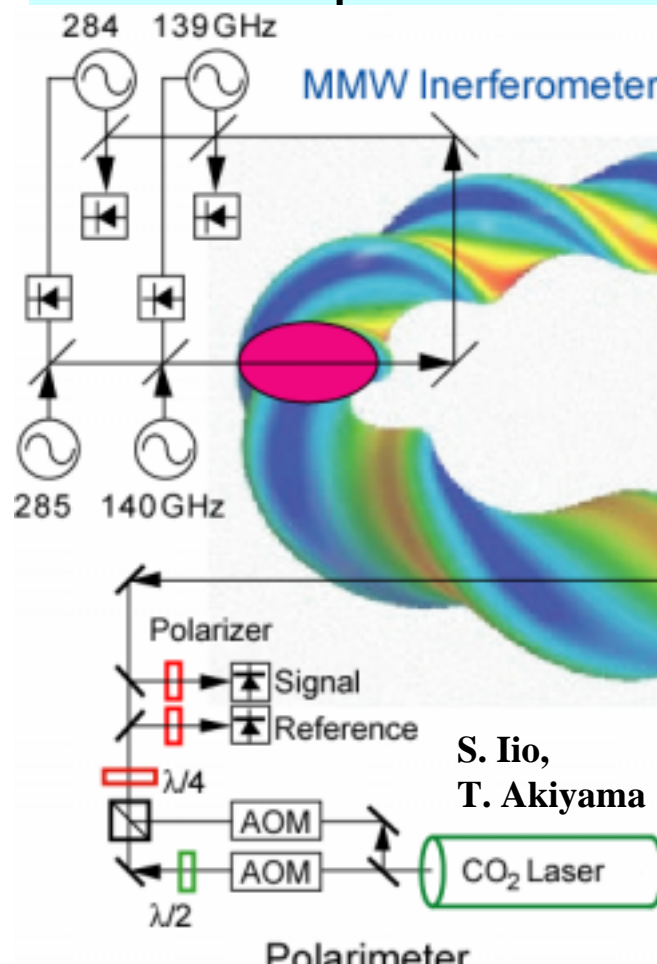
T. Ozaki, P. Goncharov, J. Lyon

T. Saida, M. Isobe, A.V. Krasilnikov, M. Sasao

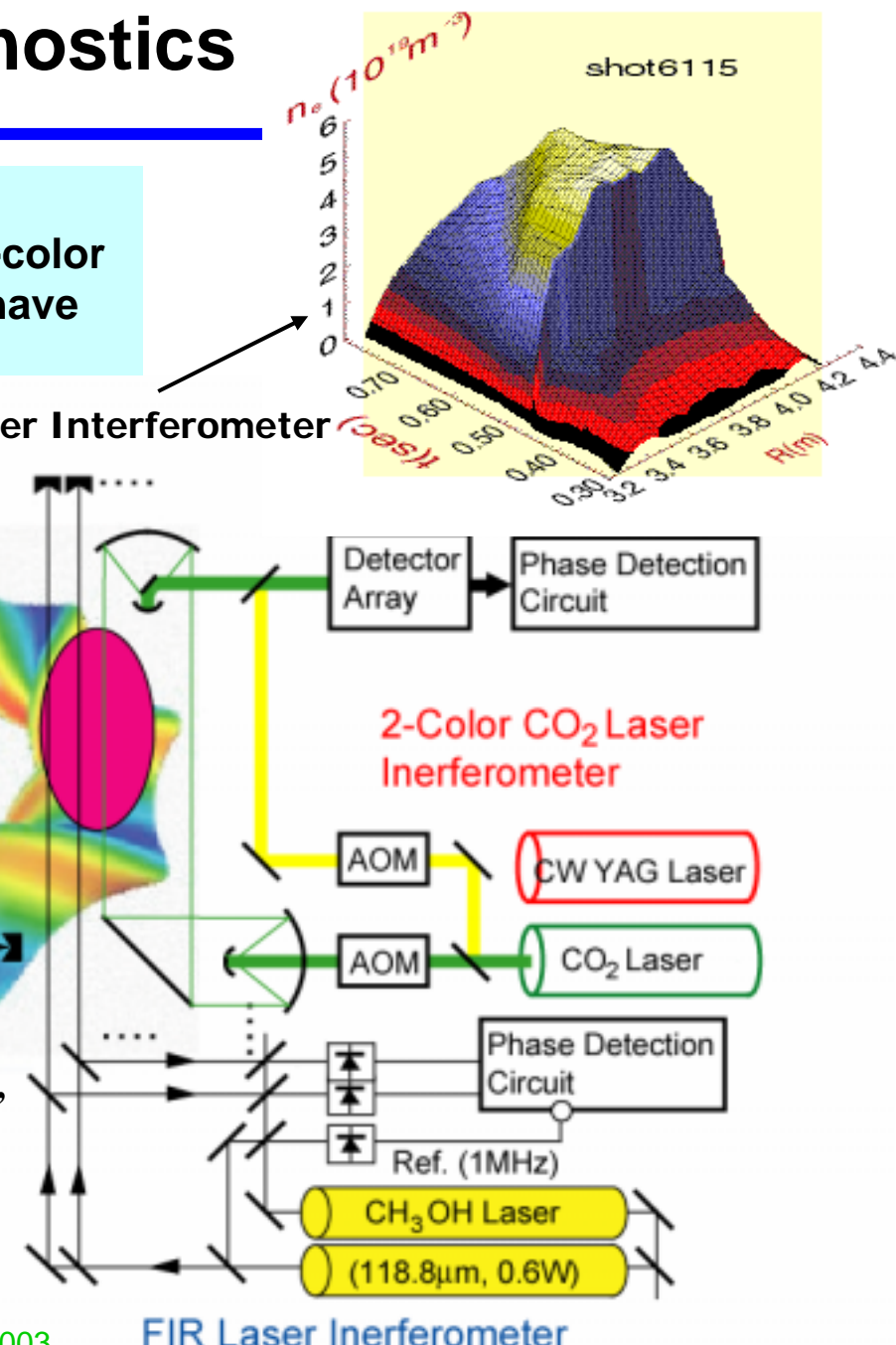


Electron Density Diagnostics

- For n_e measurement, mm-wave (MMW) interferometer, FIR laser interferometer, 2-color CO₂ laser interferometer and polarimeter have been developed in LHD.

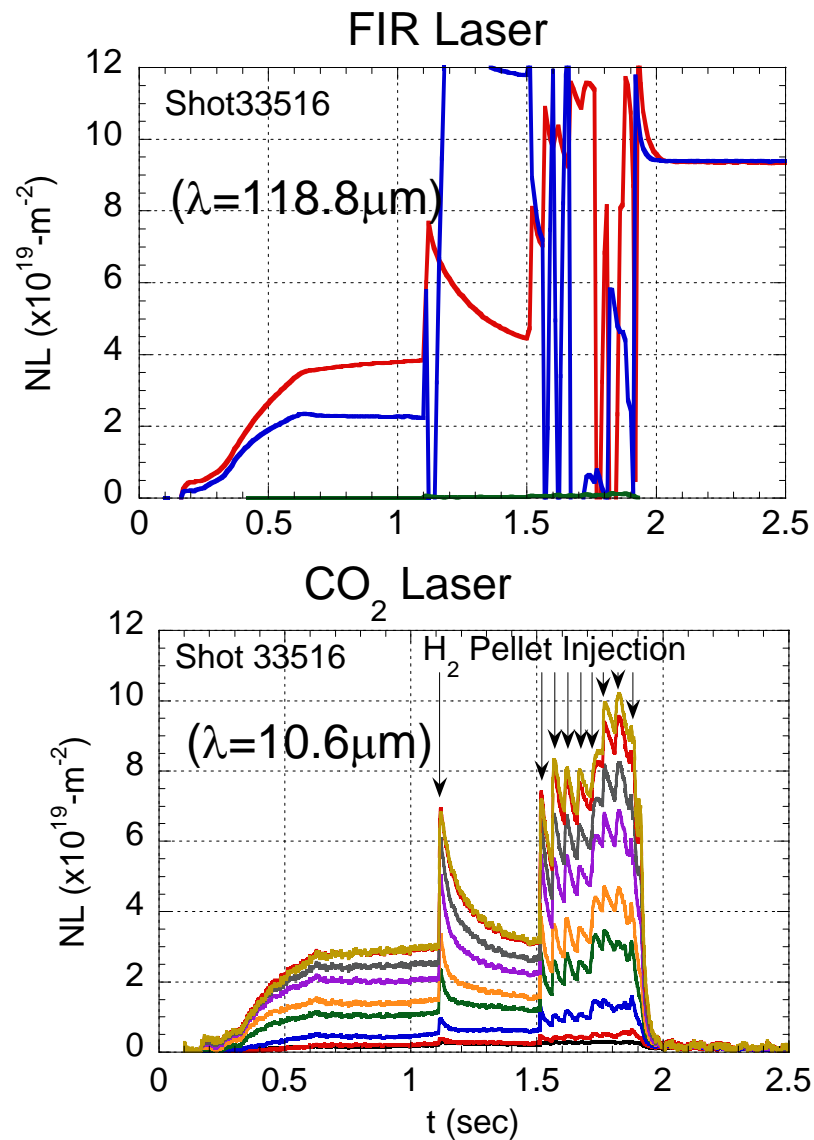
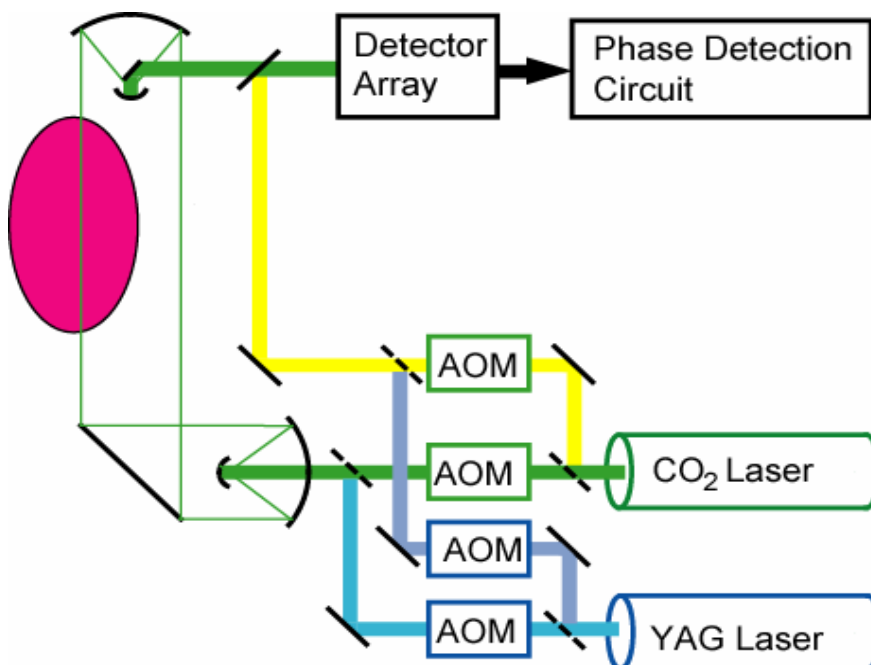


By FIR Laser Interferometer



2-Color ($\text{CO}_2 + \text{YAG}$) Laser Interferometer

- A 2-color ($\text{CO}_2 + \text{YAG}$) laser interferometer has been installed on the structure of the FIR laser interferometer in LHD.
- Even when phase jumps occur in the FIR interferometer (cf. H_2 pellets injection), phase jumps never occur in the CO_2 interferometer.



Impurity Diagnostics

9 Normal In. Monochromator (20cm)

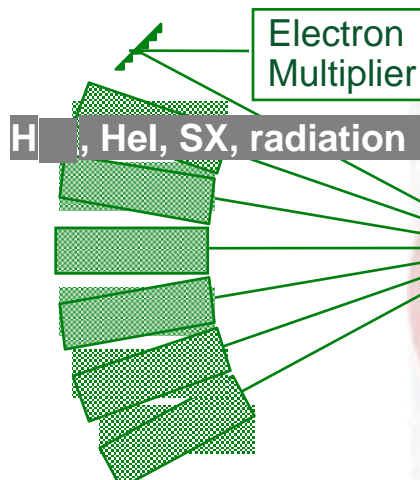
1 Grazing In. Monochromator (2.2m)

1 Normal In. Polychromator (20cm)

Impurity species are monitored with many spectrometers.

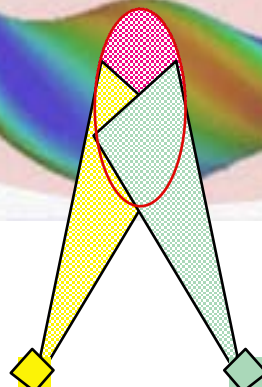
Radiation profile is monitored with bolometry.

Impurity transport is investigated with tracer pellet injection.



Impurity Monitor Station

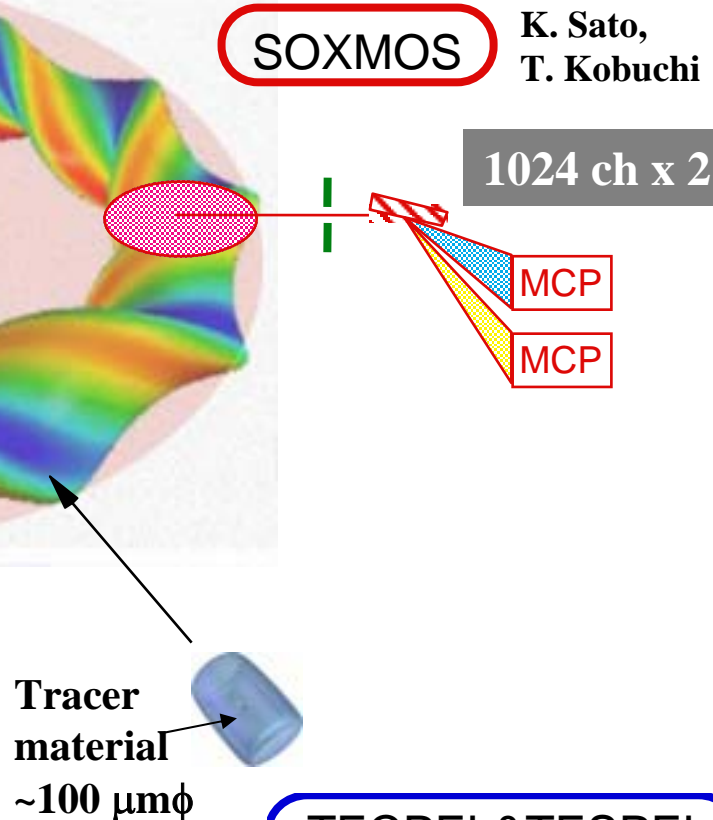
S. Morita, M. Goto



Bolometer Arrays

Imaging bolometry using
gold foil & IR camera

B.J Peterson



TECPEL&TESPEL

S. Sudo,
N. Tamura

2. Imaging Diagnostics

- Imaging diagnostics with Soft X-ray, visible spectroscopy, Imaging bolometer camera, ECE and reflectometer are being developed.

3 Imaging bolometer cameras on LHD

Well suited to steady state operation:

- (a) no electrical drift
- (b) thermal drift automatically compensated

Advantages for reactor:

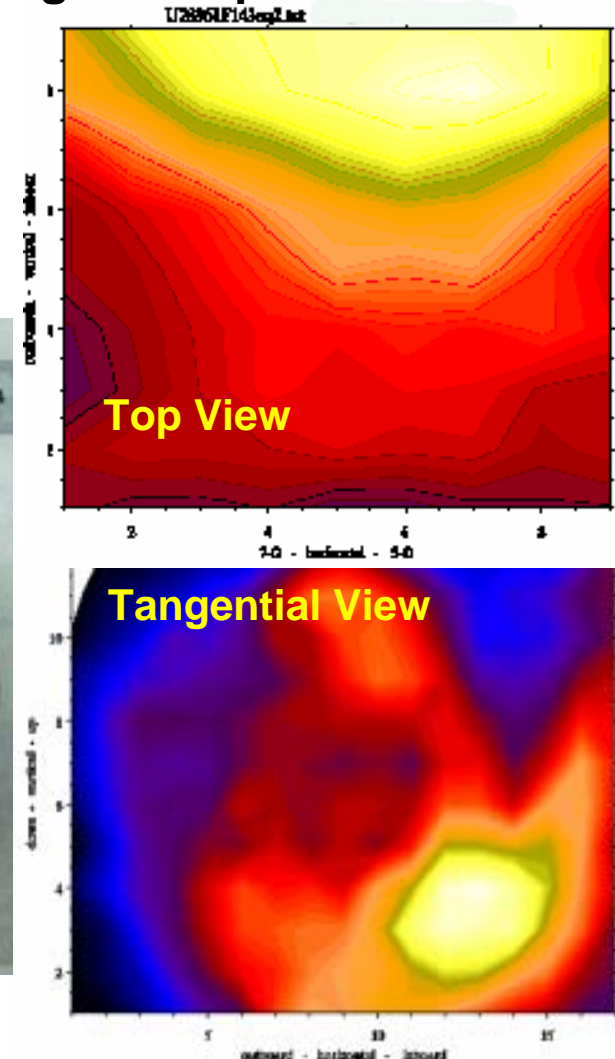
- Imaging provides hundreds of channels
- no electrical feedthroughs
- radiation hard



B. Peterson, N. Ashikawa

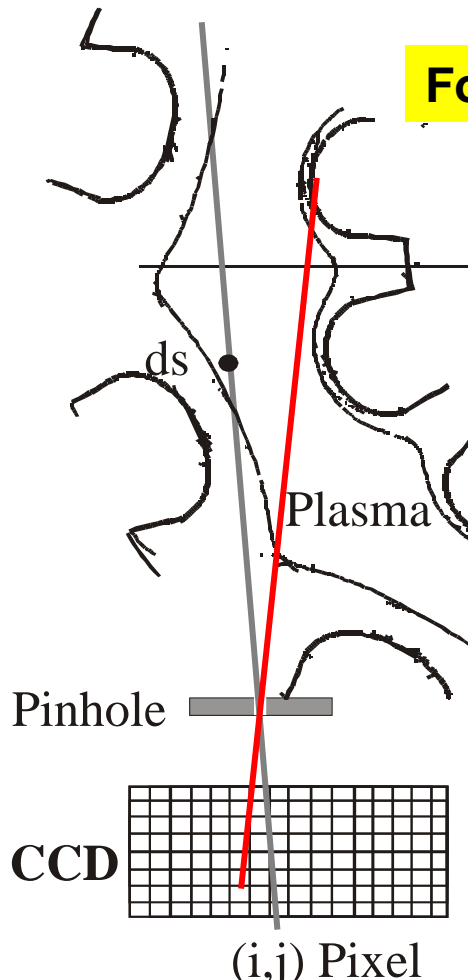
See Posters

P- 2.160, P- 4.67



Tomographic Measurement of Static Magnetic Island Using Tangential SX-CCD Camera

- Tomography of the static (2,1) magnetic island is obtained from the data of a tangential SX-CCD camera.

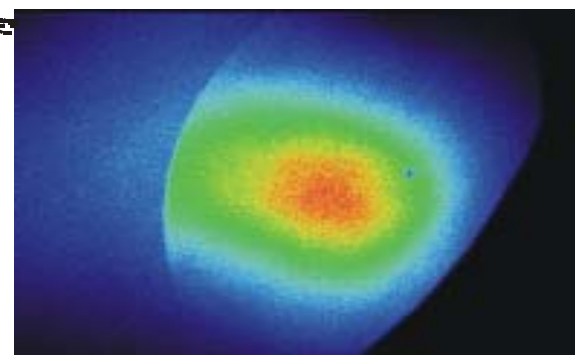


Fourier-Bessel expansion method

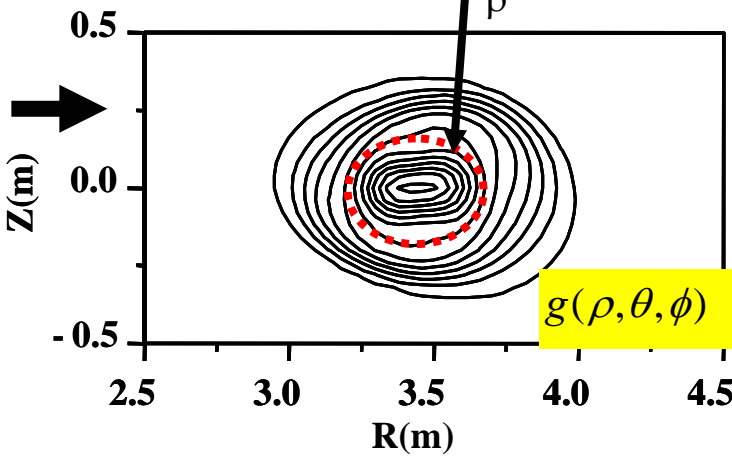
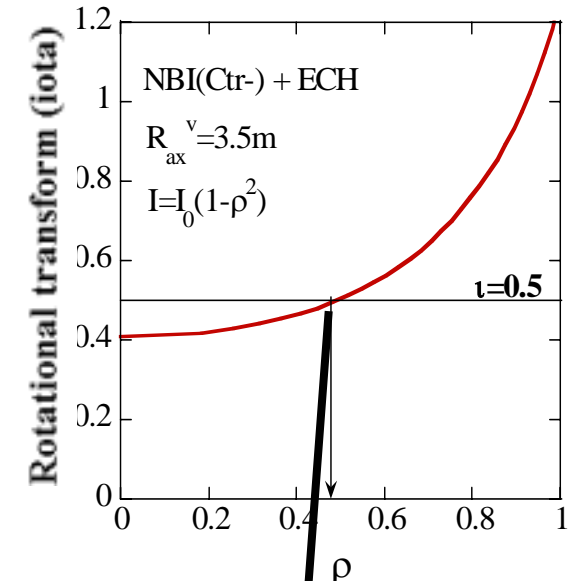
$$g(\rho, \theta, \phi) = \sum_{l=0}^L a_{0,0}^l J_0(\lambda_0^{l+1} \rho)$$

$$\begin{aligned} & + (a_{2,1}^l \cos(2\theta - \phi) \\ & + b_{2,1}^l \sin(2\theta - \phi)) J_2(\lambda_2^{l+1} \rho) \end{aligned}$$

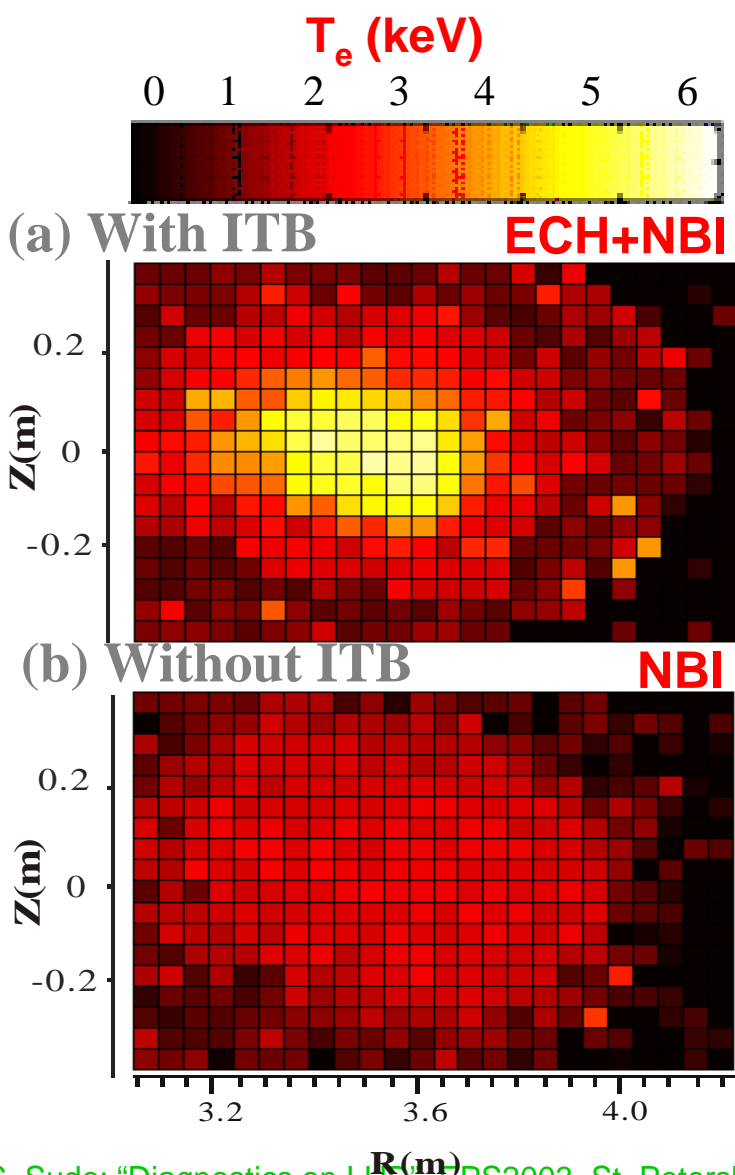
$(m,n)=(2,1)$ component



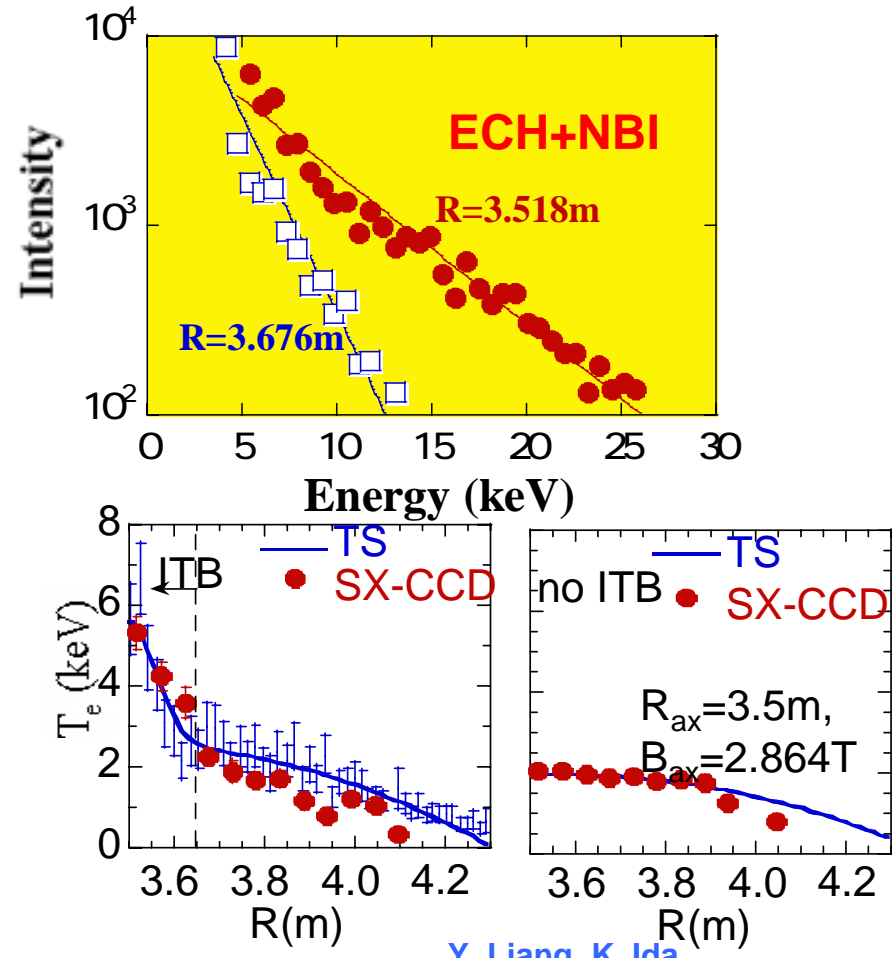
$$I_{ij}^c = \int_{P_{wall}}^{P_{pinhole}} g(\rho, \theta, \phi) ds$$



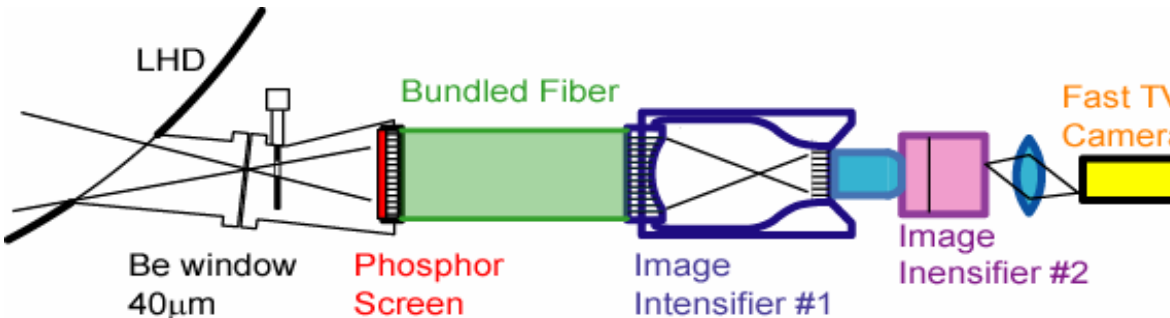
2D T_e measurement using X-ray CCD



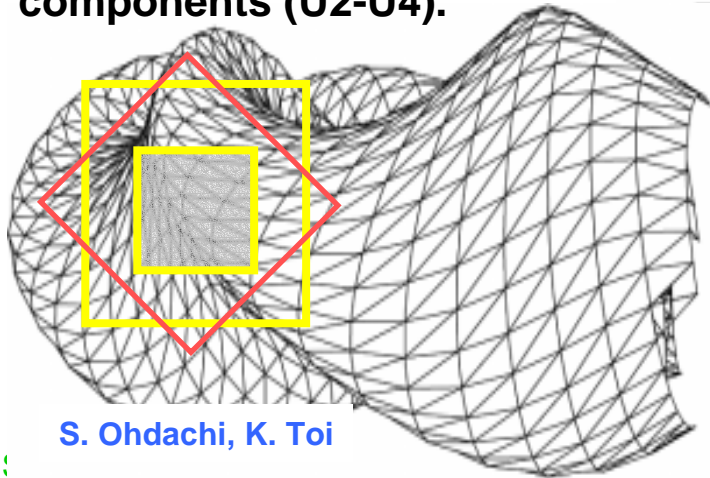
- By using photon counting with a X-ray CCD, the 2-D T_e profile can be measured.
- Comparison is done for the plasmas with and without ITB in LHD.



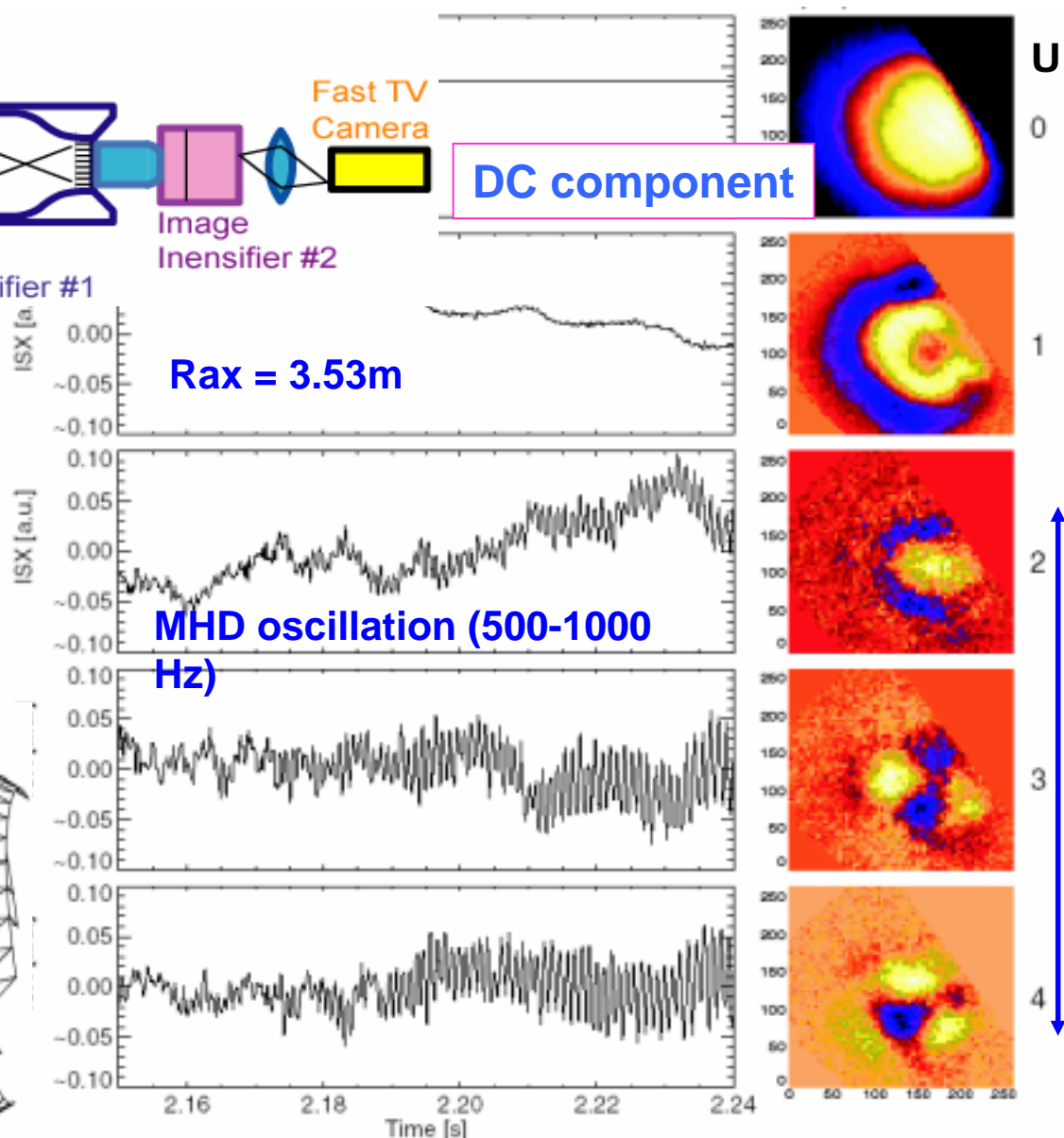
Fast SX-TV Camera Observing m=2 MHD Mode Structure



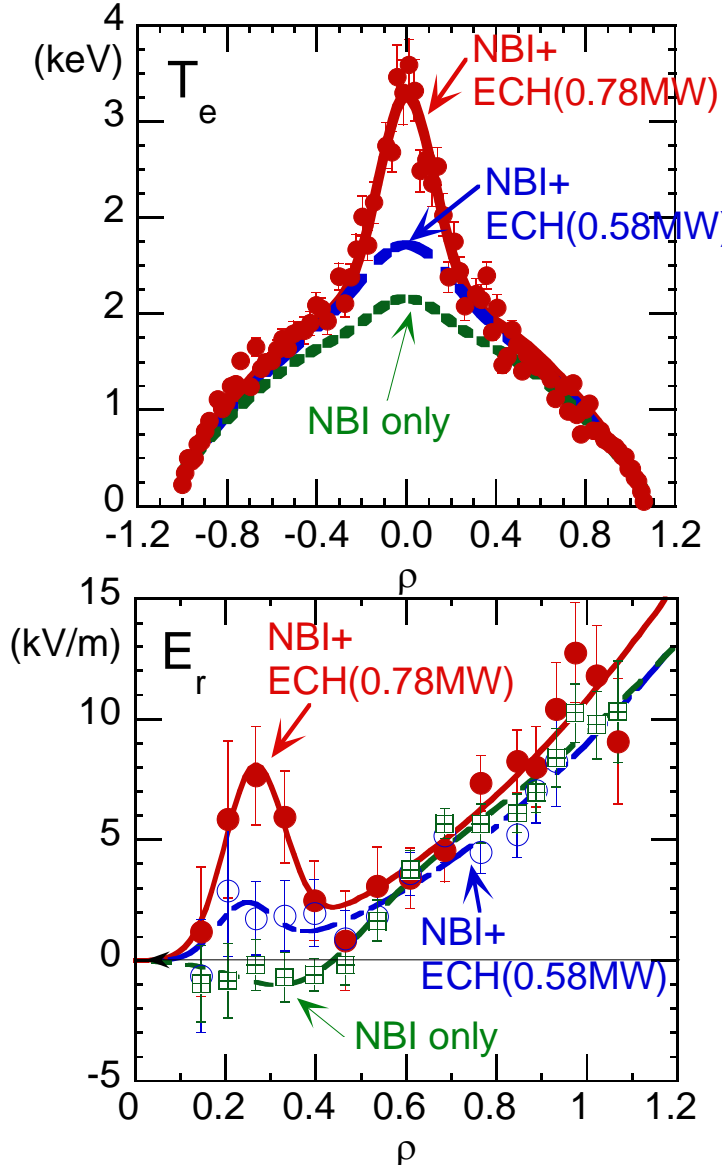
- SX image is tangentially measured by fast TV camera (4,500 frames/sec) coupled with the image intensifier.
- Singular Value Decomposition technique is used to extract the rotating $m = 2$ structure with constructing from three components (U_2-U_4).



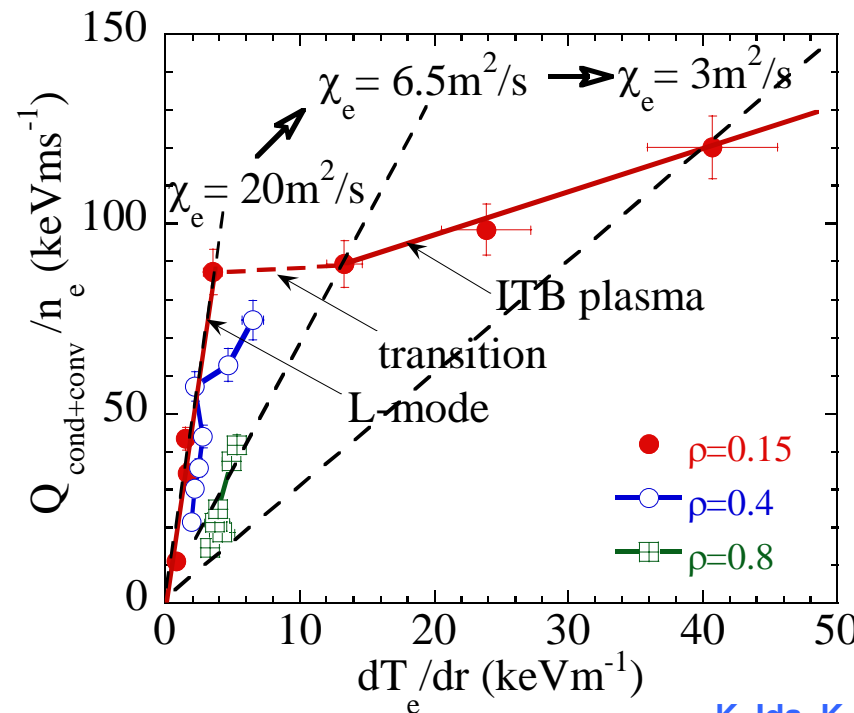
S. Ohdachi, K. Toi



3. Electric Field Diagnostics

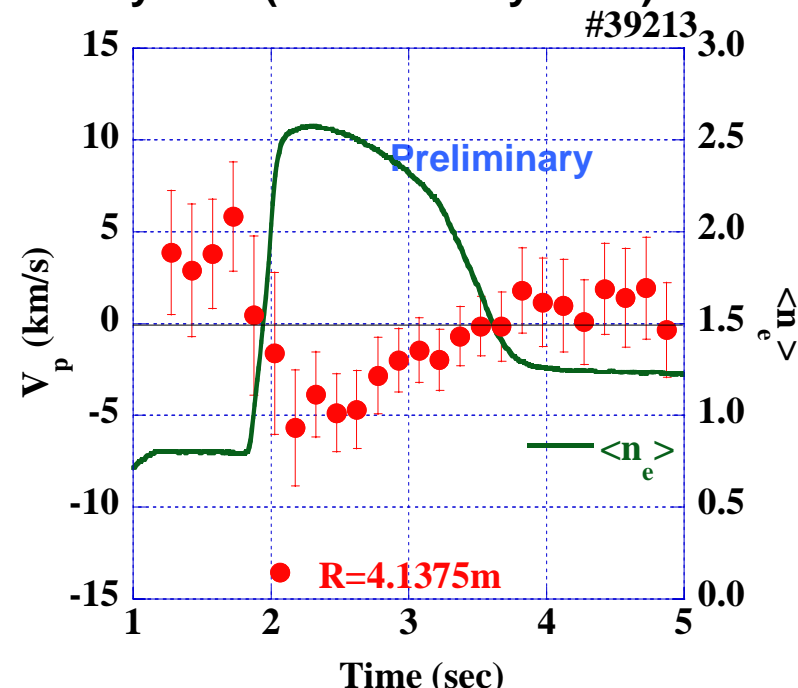
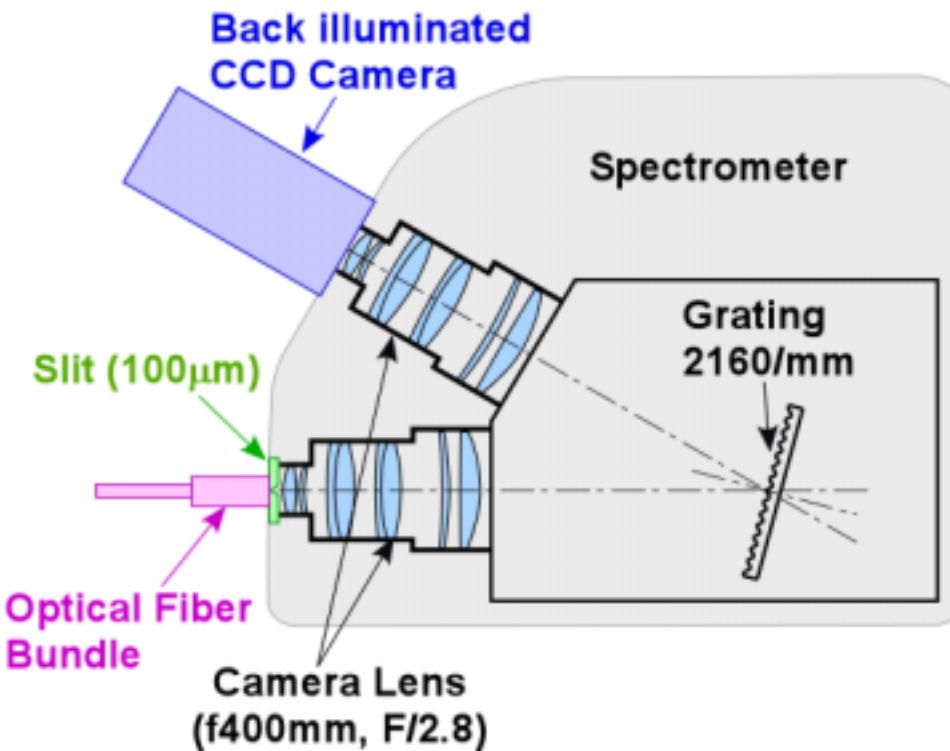


- Radial electric field is a key to understand a helical plasma and especially ITB, and it is measured by CXS.
- Radial electric field has a reversed gradient at the ITB, which is generated by the ECH in LHD.
- Clear transition from L to ITB is observed.
- The χ_e is reduced to 1/30 of L-mode after the ITB transition.



Fast CXS measurement for E_r

- Fast CXS has been developed to study phase transition of ITB in LHD.
- Time resolution of poloidal rotation velocity was improved from 500ms to 100 ms.
- High throughput spectrometer
 - Large diameter camera Lens - F/2.8 (Traditionally F/5.6)
 - Back illuminated CCD Camera - Quantum Efficiency 80% (Traditionally 25 %)



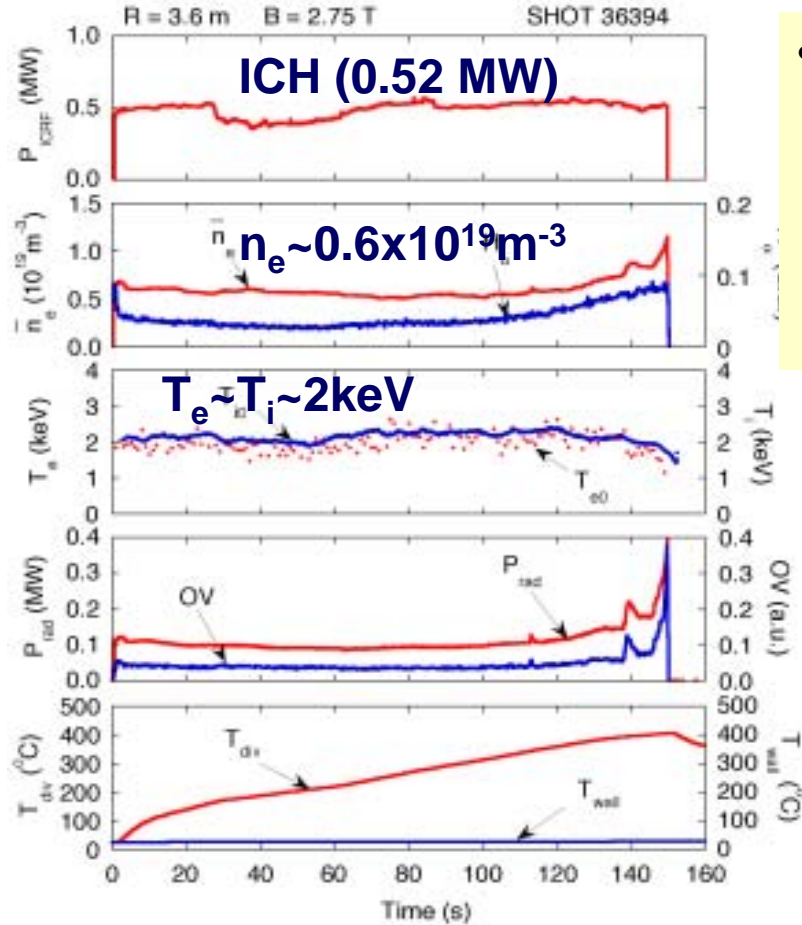
The 6MeV HIBP accelerator operation has been officially approved! → HIBP testing.

S. Sudo: "Diagnostics on LHD", EPS2003, St. Petersburg, 77-11/2003.

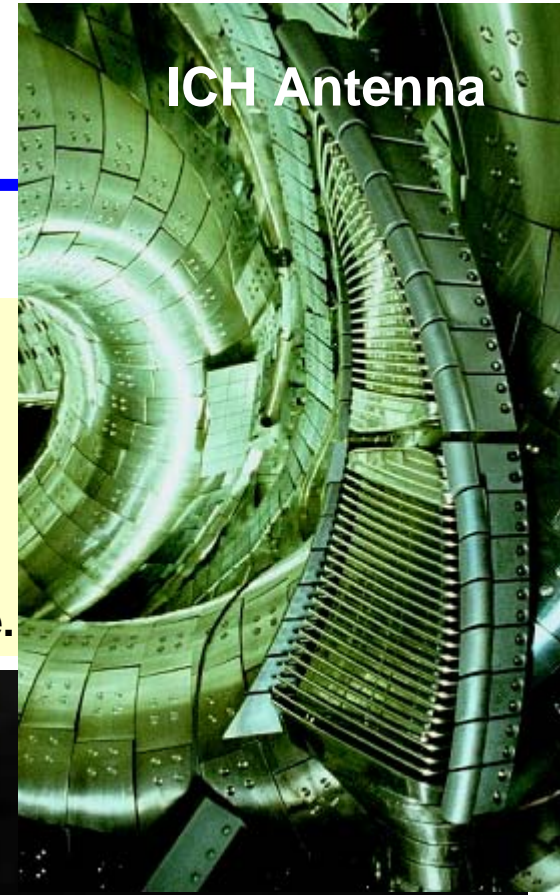
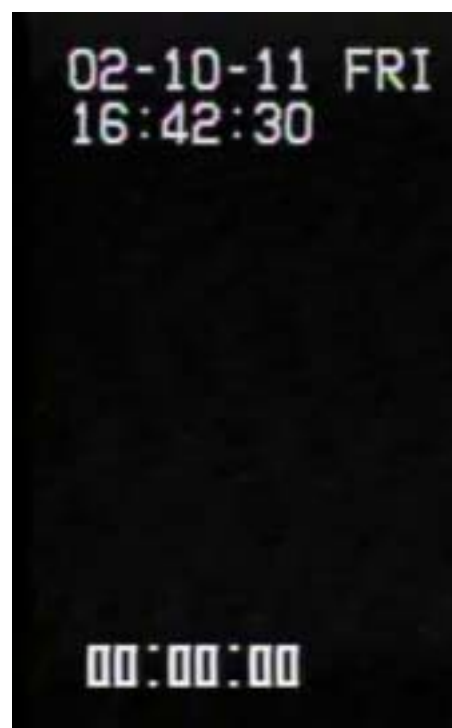
Time evolution of poloidal rotation velocity and line averaged electron density.

4. Long Pulse Plasma Operation

- Long pulse plasma (150 s) is sustained by ICH.



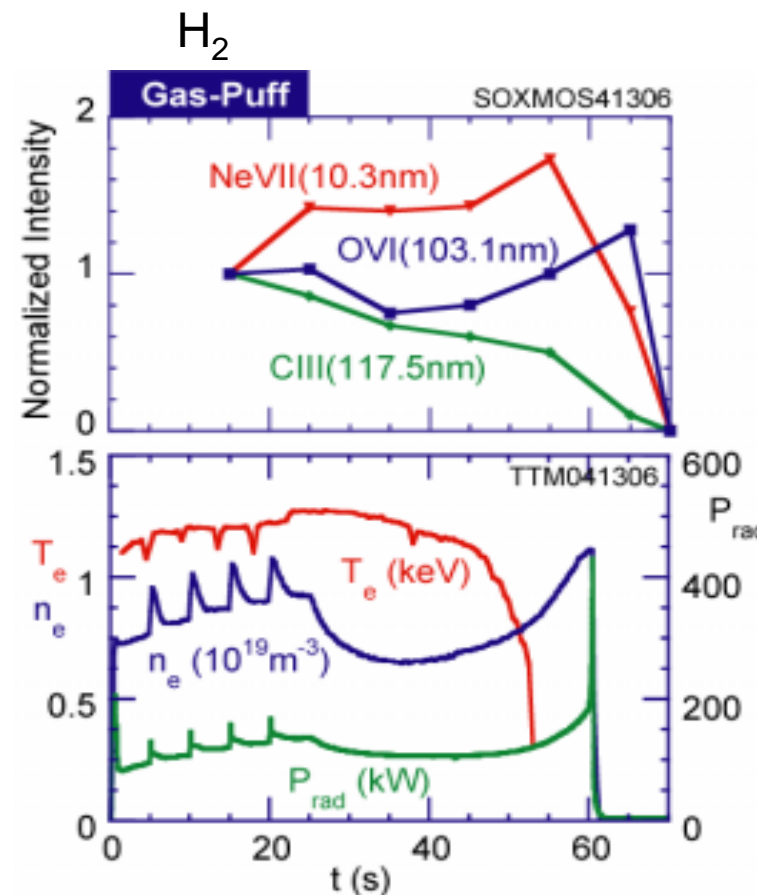
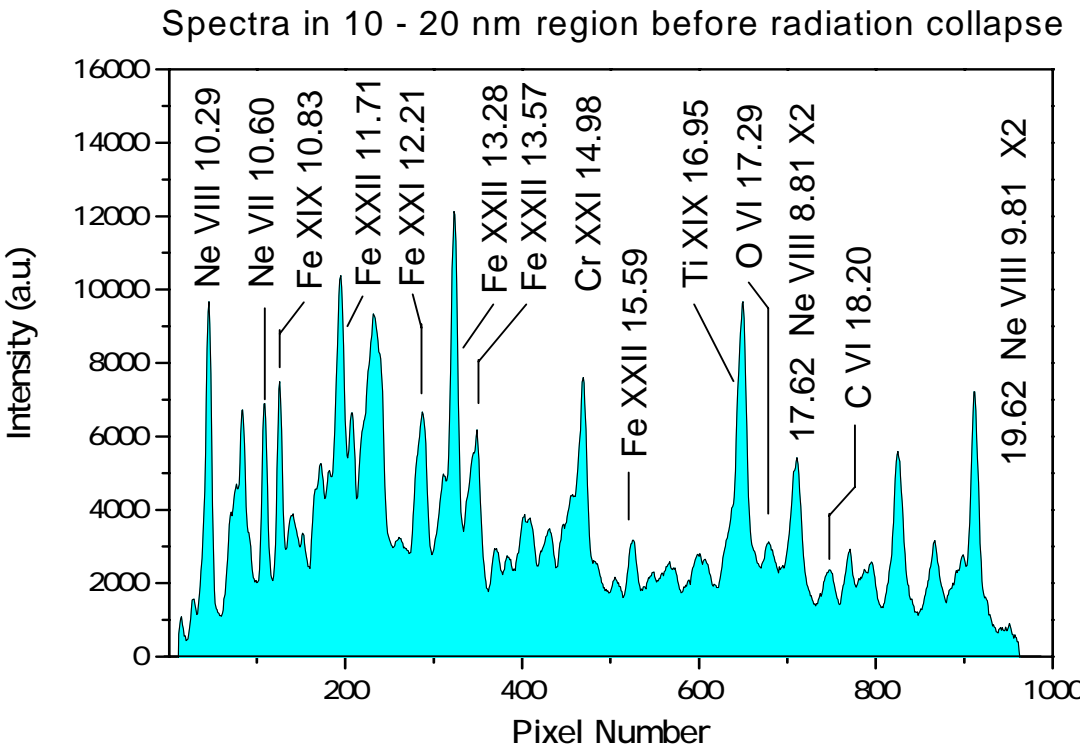
- Gradual increase of n_e , H_α , P_{rad} after 100s [outgassing from graphite divertor tiles] due to wall temperature increase.



The basic diagnostics are working well also for the long pulse operation.

Observation of recycling effect with SOX-MOS

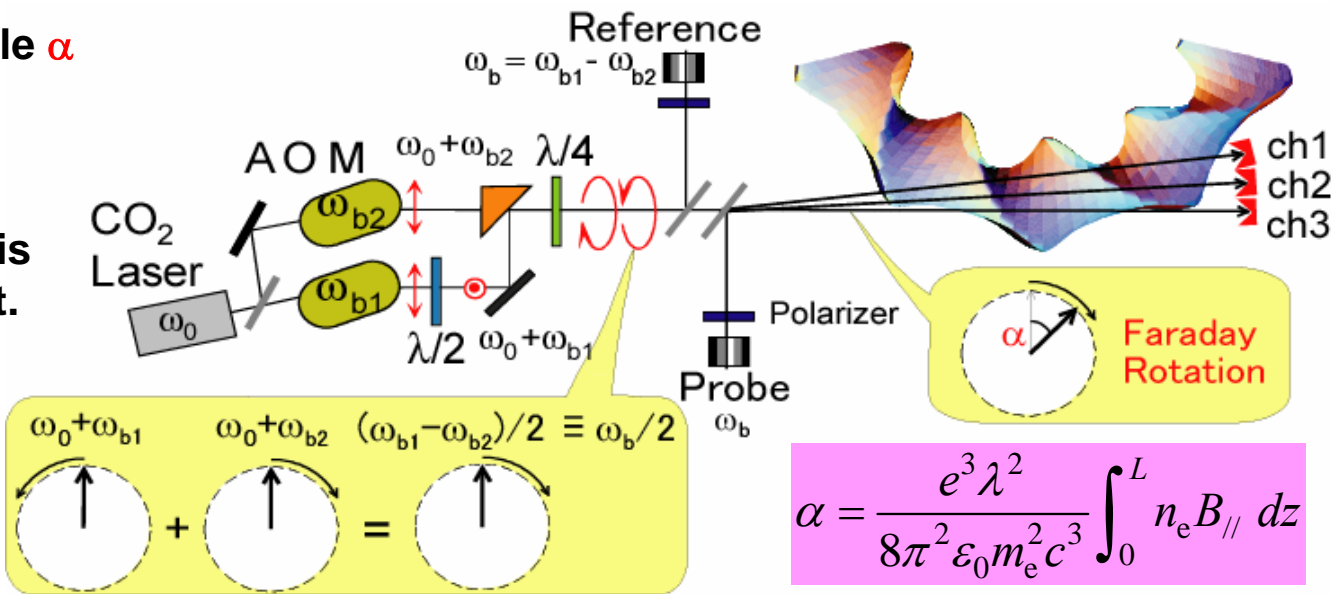
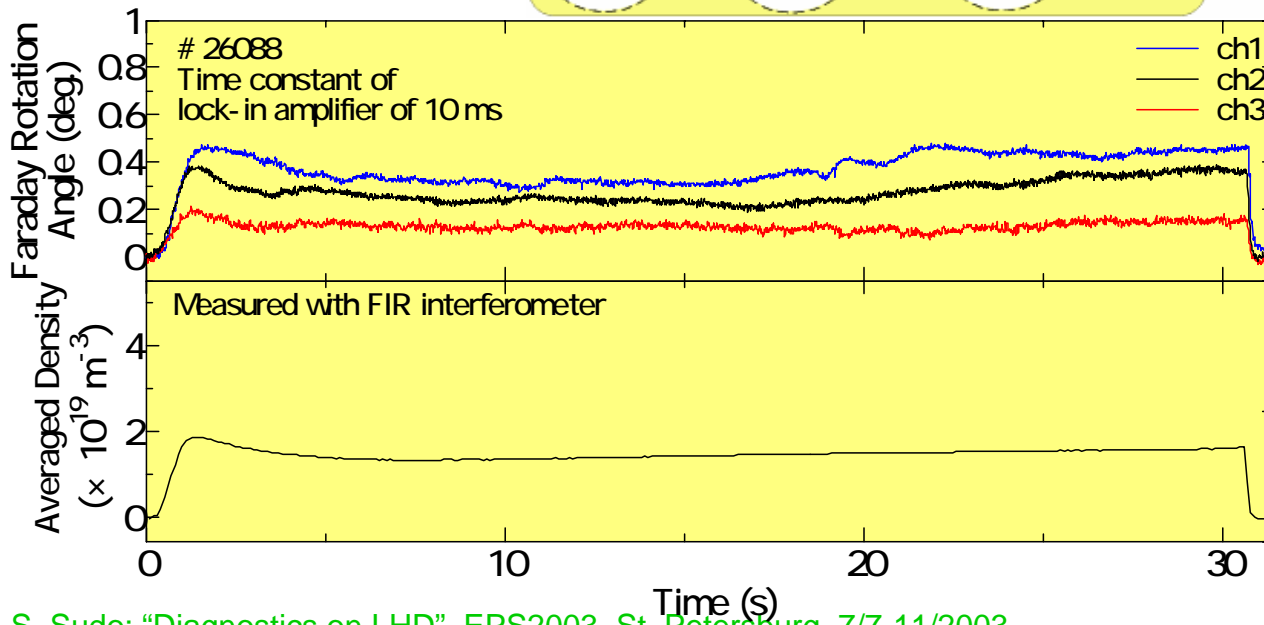
- SOX-MOS spectrometer indicates that Ne and O gas comes out from the wall and causes radiation collapse. This experiment was done after the heavy neon glow discharge cleaning.
- The desorption of the gas, which is adsorbed on the walls, occurs in the late phase of the plasma discharge.



Polarimetry for n_e in steady state operation

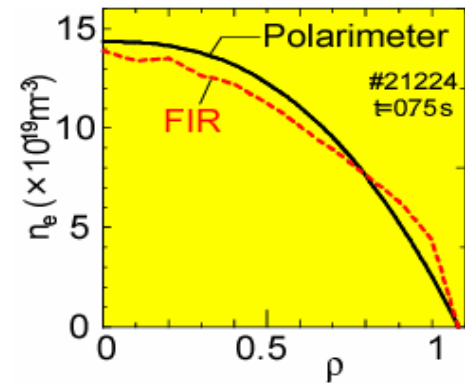
The Faraday rotation angle α is detected as the phase difference between reference and probing signals, and this system is free from fringe miscount.

Polarimetry with CO₂ laser is reliable, and refraction is small.



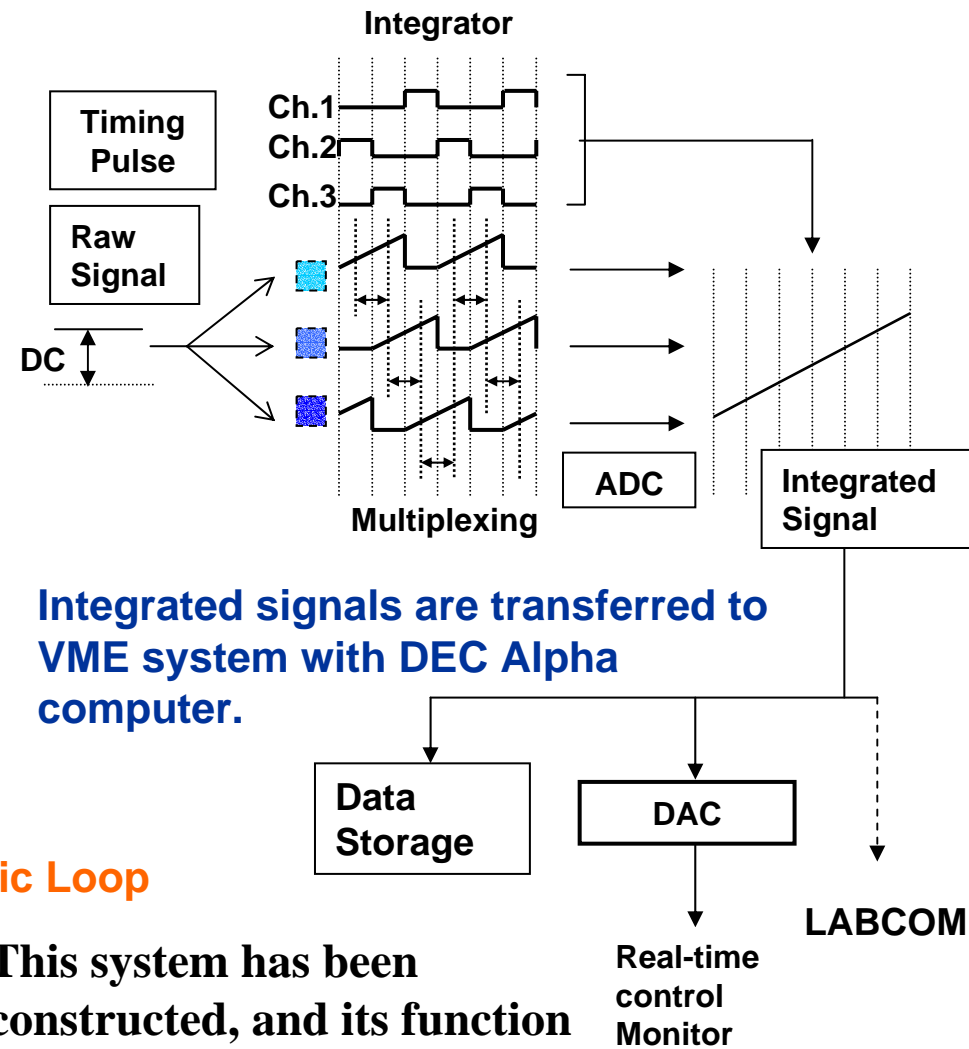
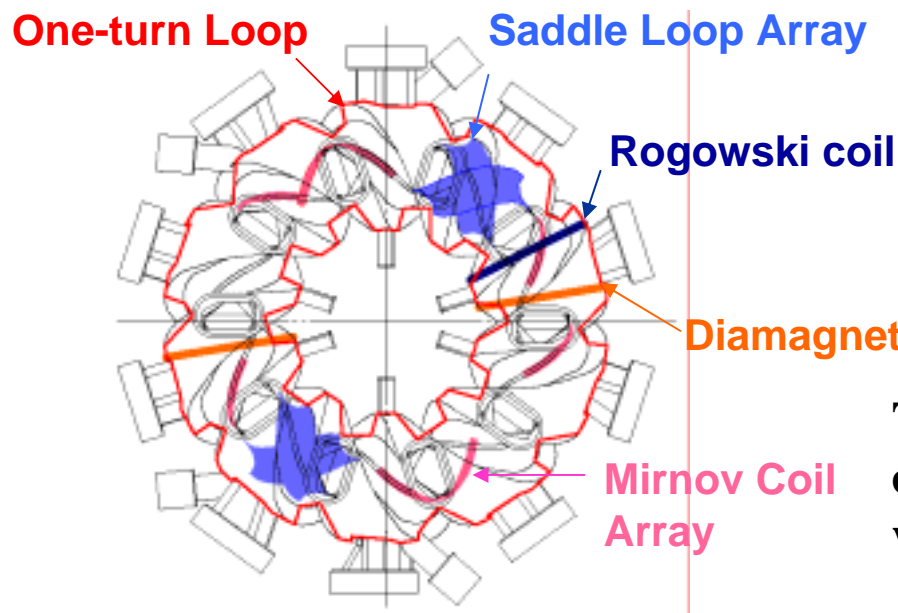
$$\alpha = \frac{e^3 \lambda^2}{8\pi^2 \epsilon_0 m_e^2 c^3} \int_0^L n_e B_{\parallel} dz$$

$$n_e(\rho) = a \left\{ 1 - (\rho / \rho_B)^b \right\}$$



Magnetics for Steady State Plasma

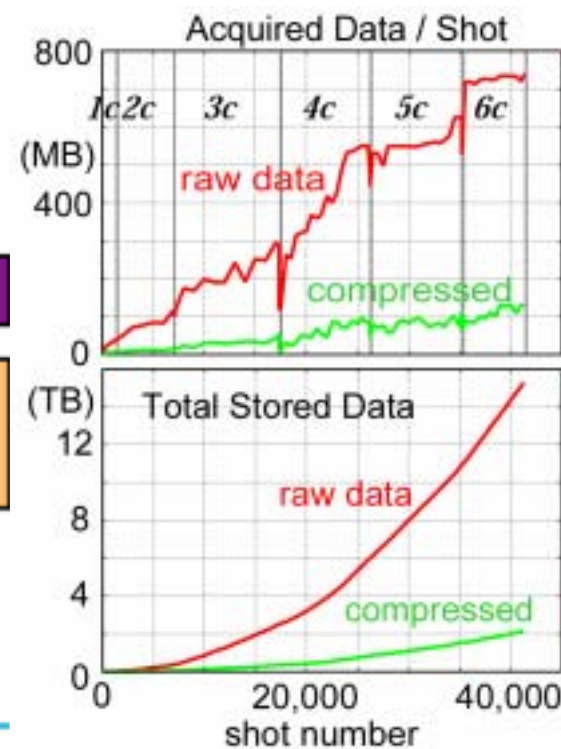
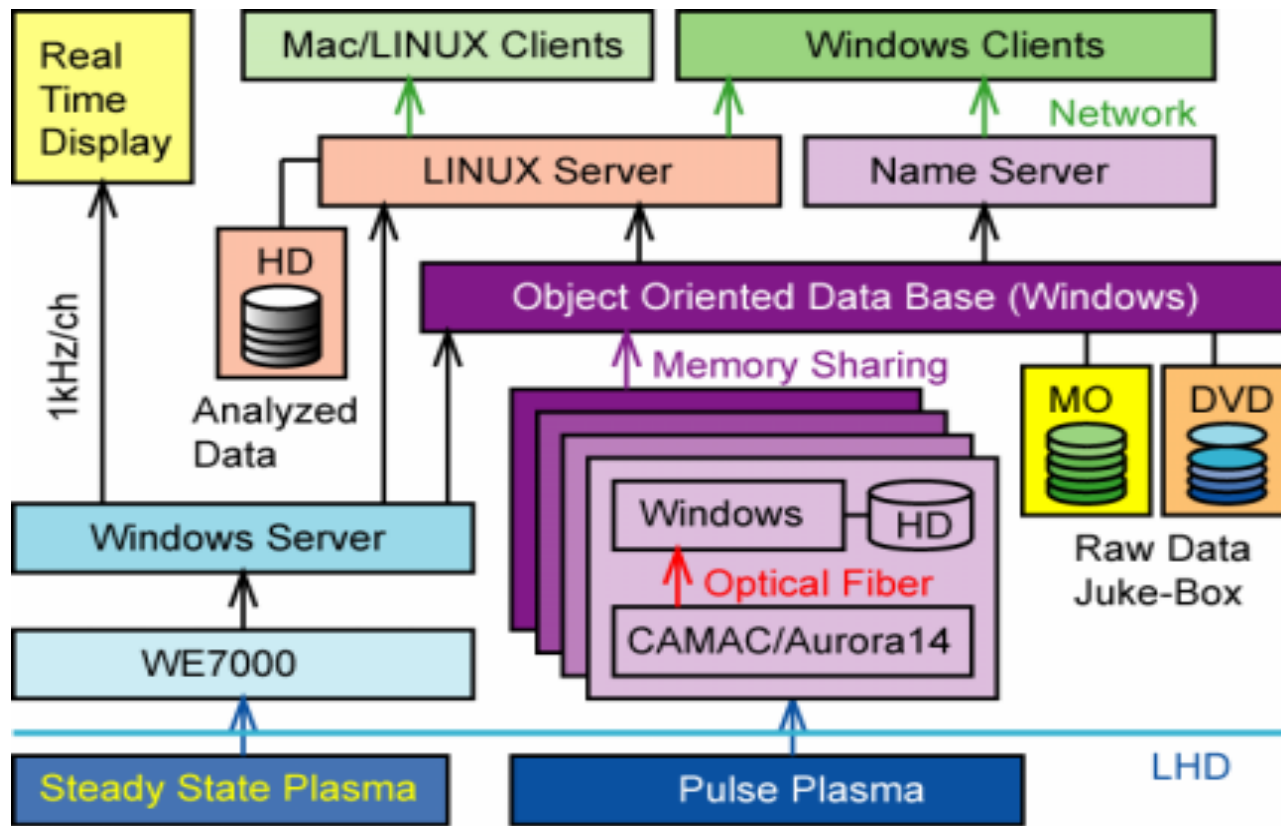
- New-type integrator using three operational amplifiers has been developed for steady state operations.
- The integrator avoids saturation of integrated signal linearity of thermal drift in short-time integration.



S. Sakakibara

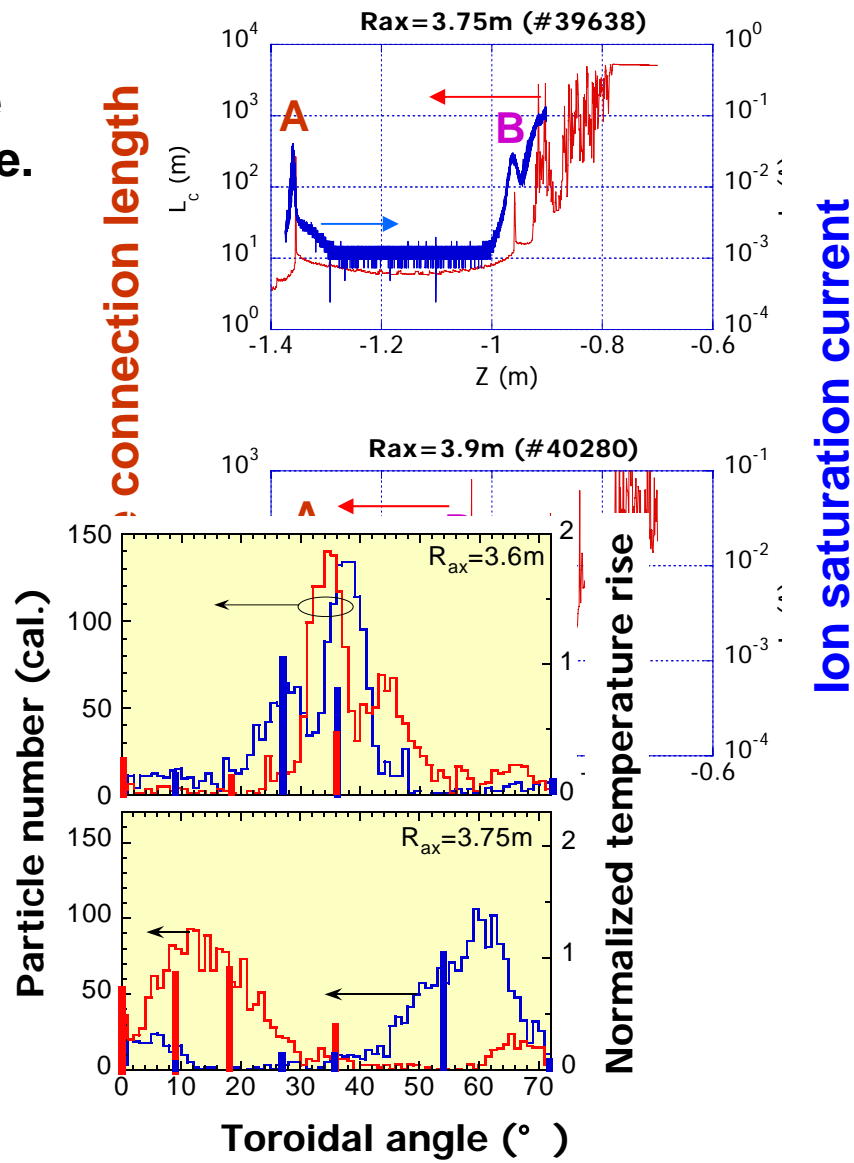
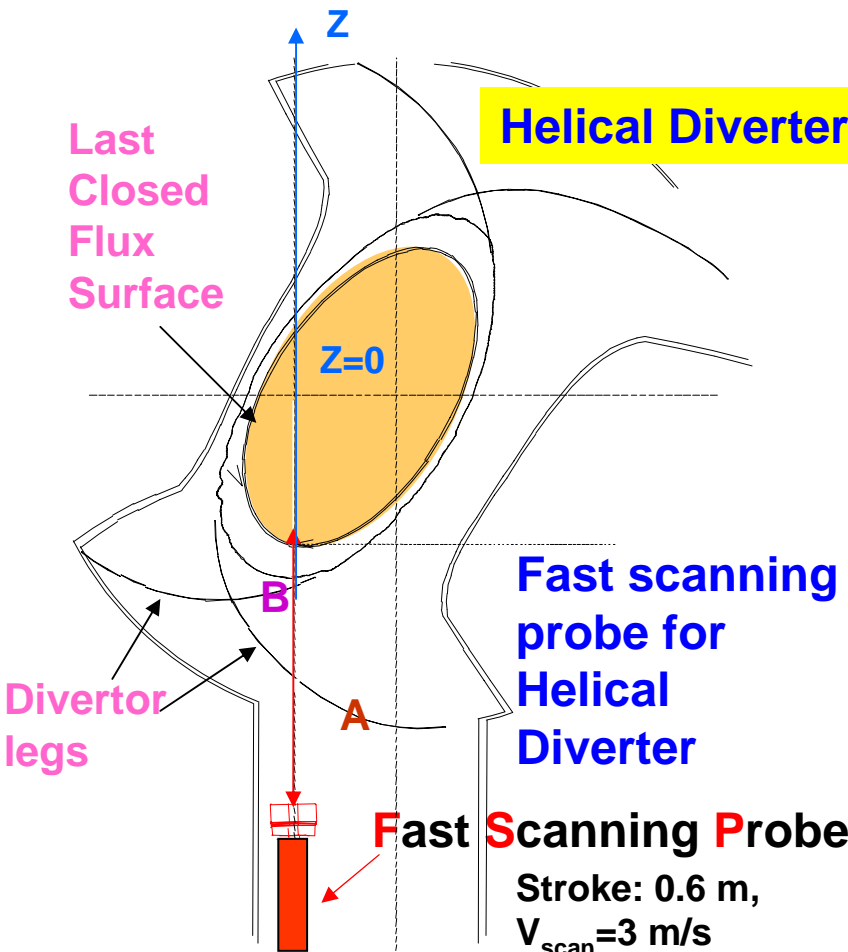
Data Acquisition and Storage/Retrieval

- Basic Data of steady state plasma are displayed in real time.
- Acquired data are increasing and data of 15TB have been stored.
- Big raw data are successfully managed using object oriented data base.
- Analyzed data are served by LINUX servers. **740 MB/shot, 150 shots/day**



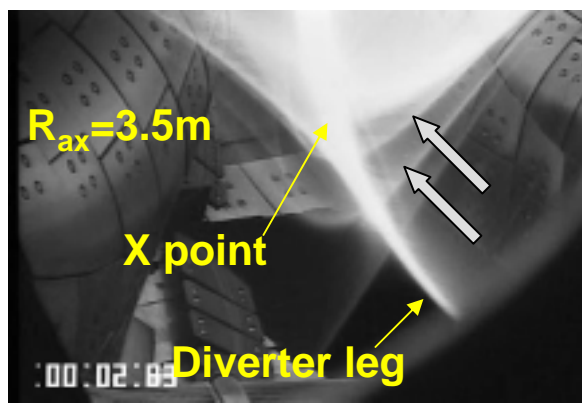
5. Diagnostics for Edge and Divertor Plasmas

- Peak positions of ion saturation current profile agree well with those of field line connection length profile.



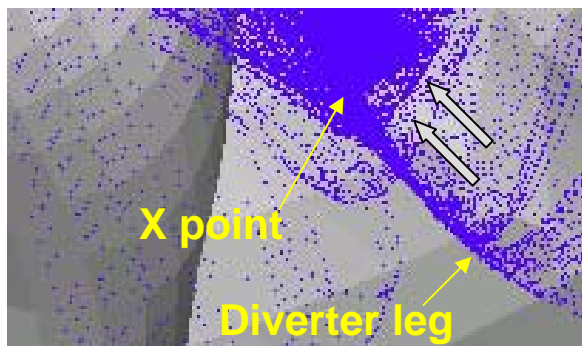
- Locations of neutral emission are determined using Zeeman effect, since the magnetic field is different at different positions on the same line of sight. It is also confirmed that the line emission is localized.
- Emission comes from the divertor surface as confirmed by H α TV image.

H plasma



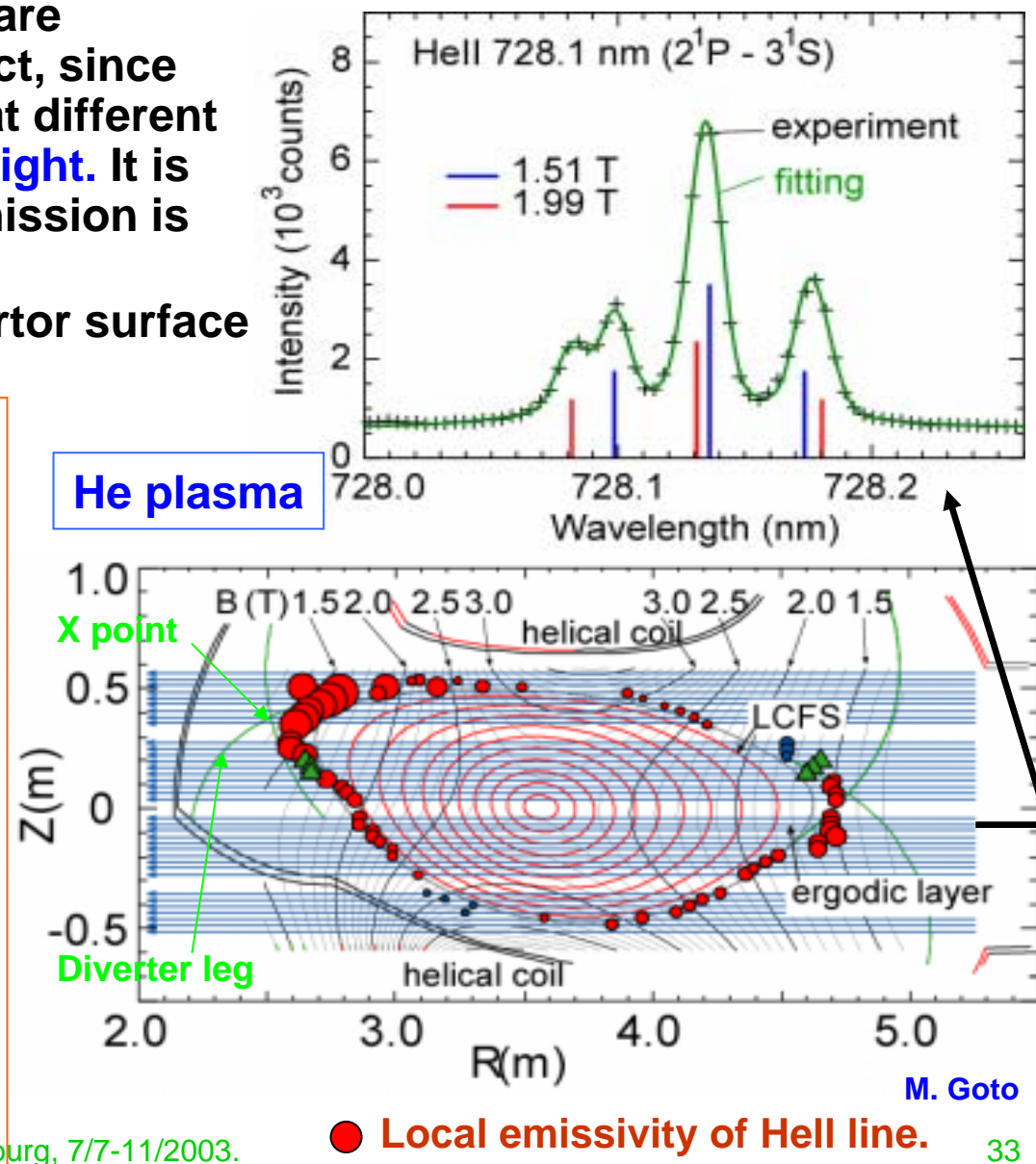
H α
CCD TV
camera

Field
line
tracing

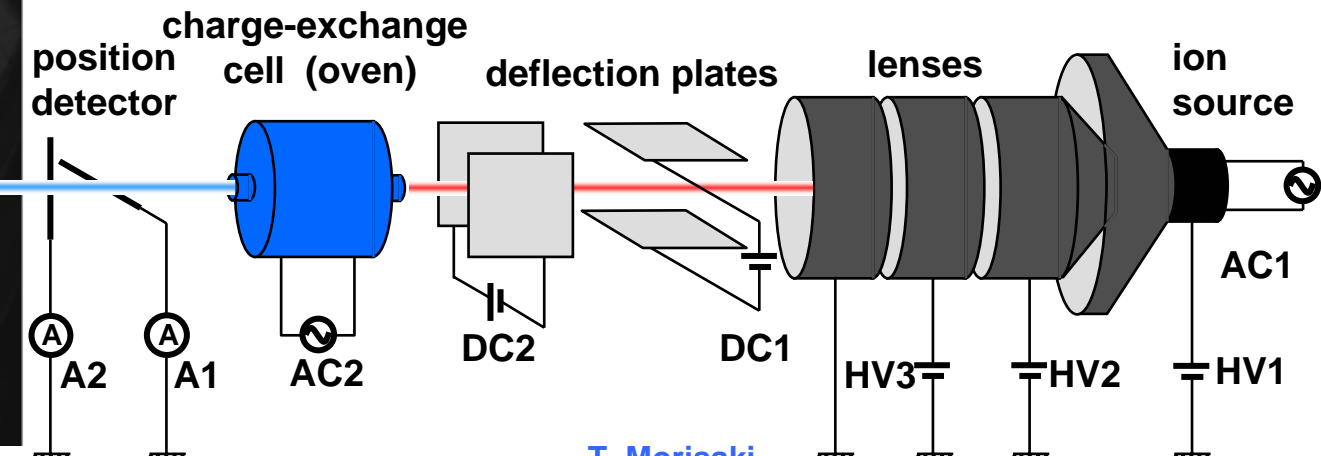
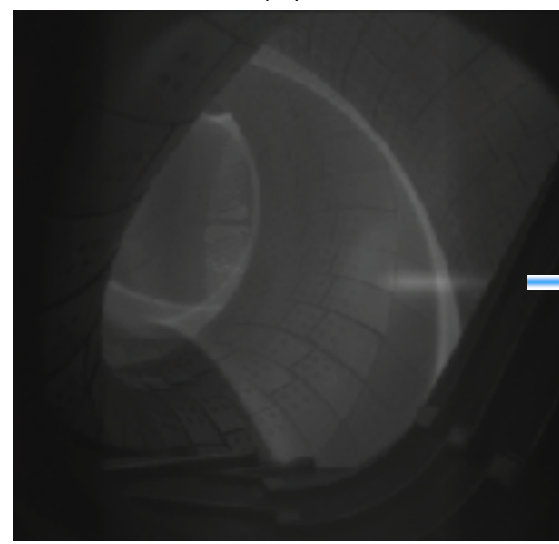
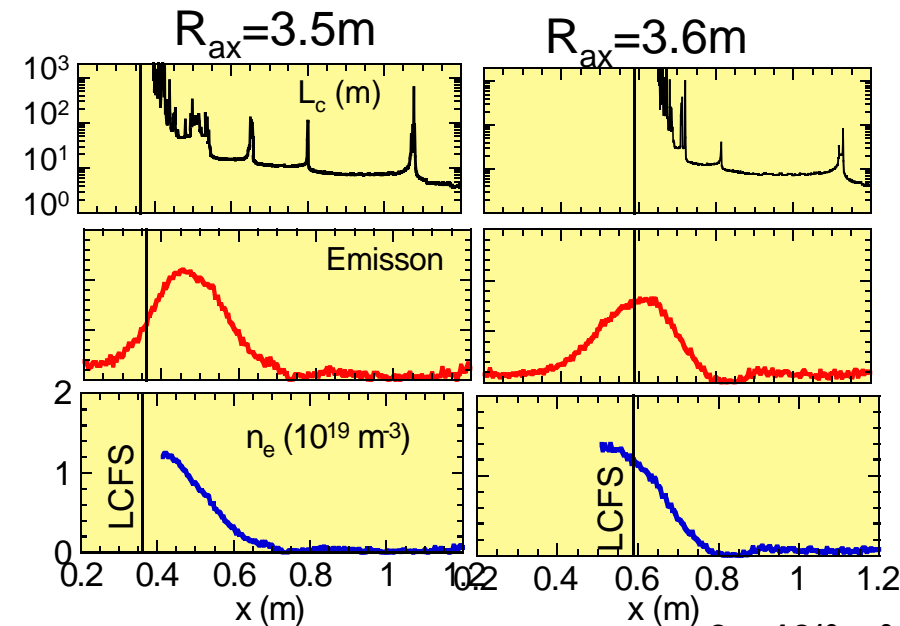


M. Shoji

S. Sudo: "Diagnostics on LHD", EPJ-S2003, St. Petersburg, 7/7-11/2003.

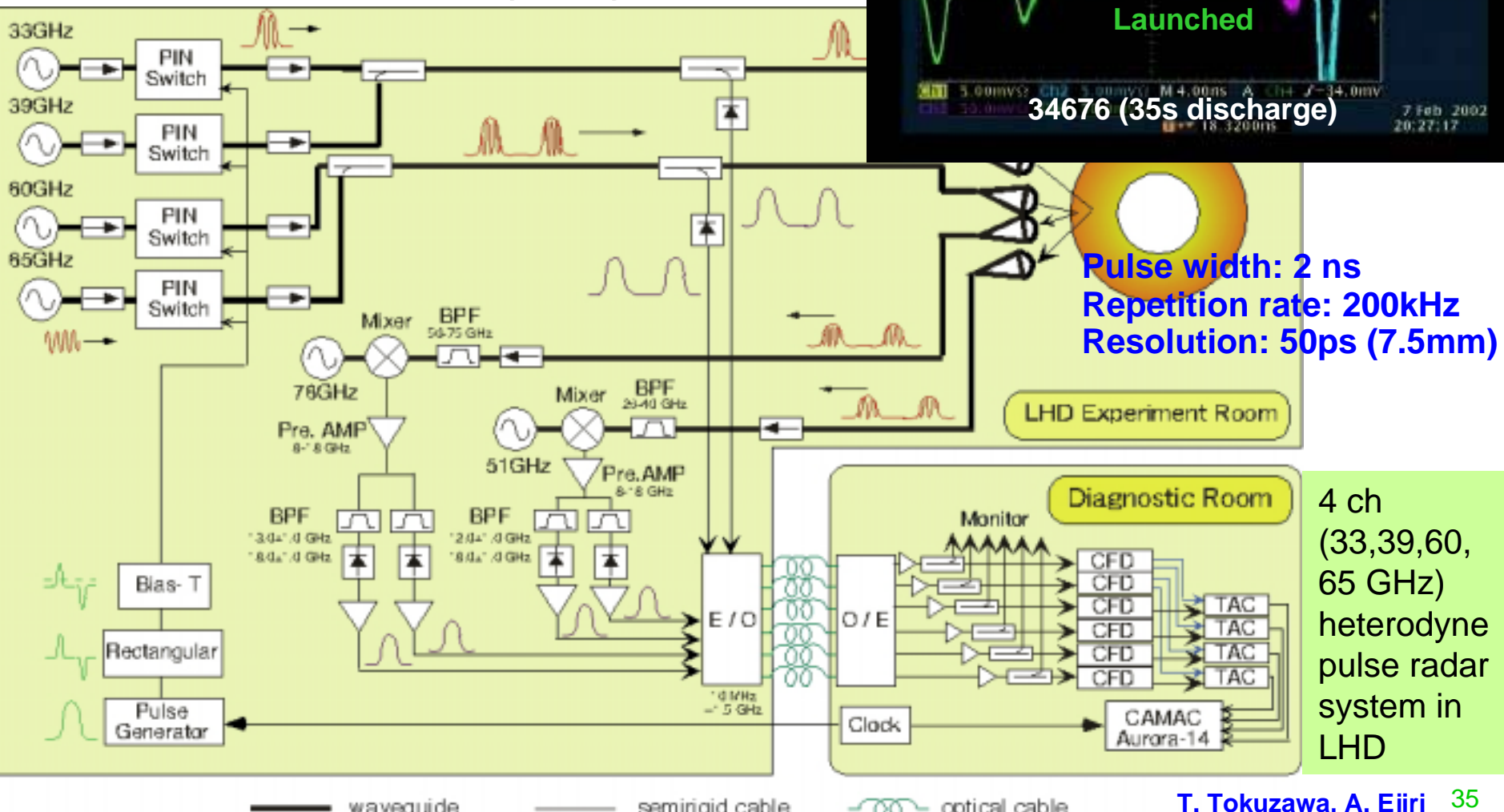


Measurement of edge n_e by Lithium Beam Probe



Pulse radar reflectometer for n_e profile & fluctuation at the edge

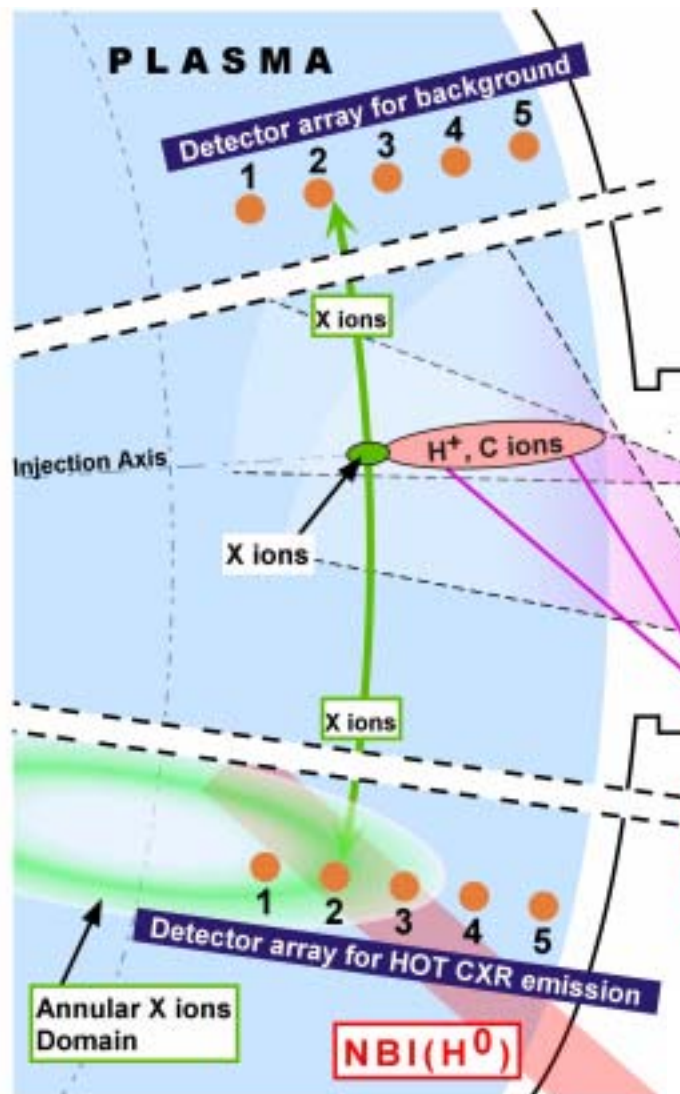
- Pulsed radar reflectometer is useful to measure the n_e profile and fluctuation in the edge region.



6. Innovative Diagnostics

through international collaboration

Tracer-Encapsulated Solid Pellet (TESPEL)



Developed for advanced particle transport study. Tracer particles, such as Li, Ti, can be deposited locally inside the plasma.

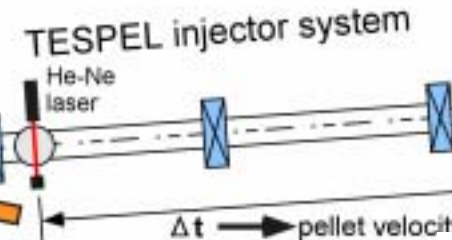
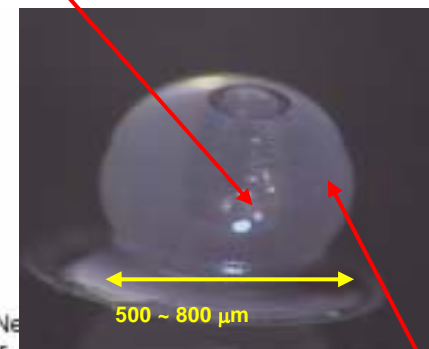


Photo detectors
for confirmation
of the tracer
local deposition

Tracer particle

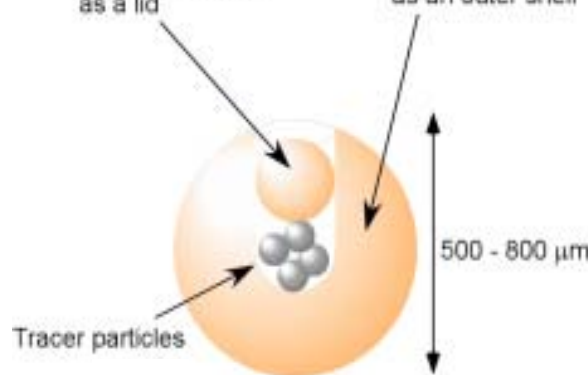


Polystyrene
(C_8H_8)_n

Polystyrene (C_8H_8)_n

as an outer shell

Polystyrene ball
as a lid



*S. Sudo, N. Tamura, D. Kalinina, V. Sergeev, B. Kuteev,
A. Matsubara, I. Viniar, K. Sato, D. Stutman, M. Finkenthal*

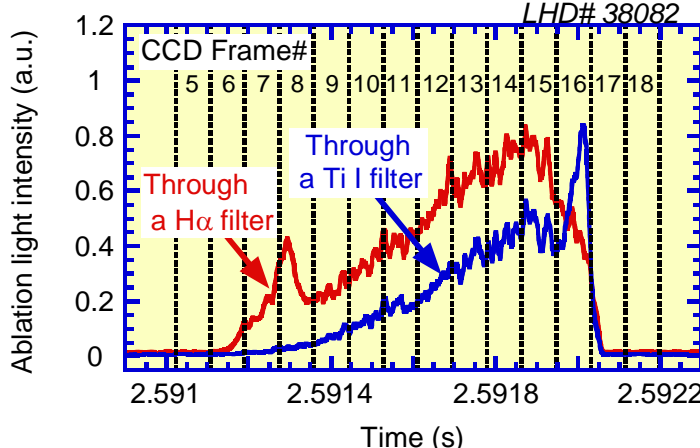
Spectra of Light Emissions from TESPEL Ablated Cloud

With Fast CCD + Spectrometer

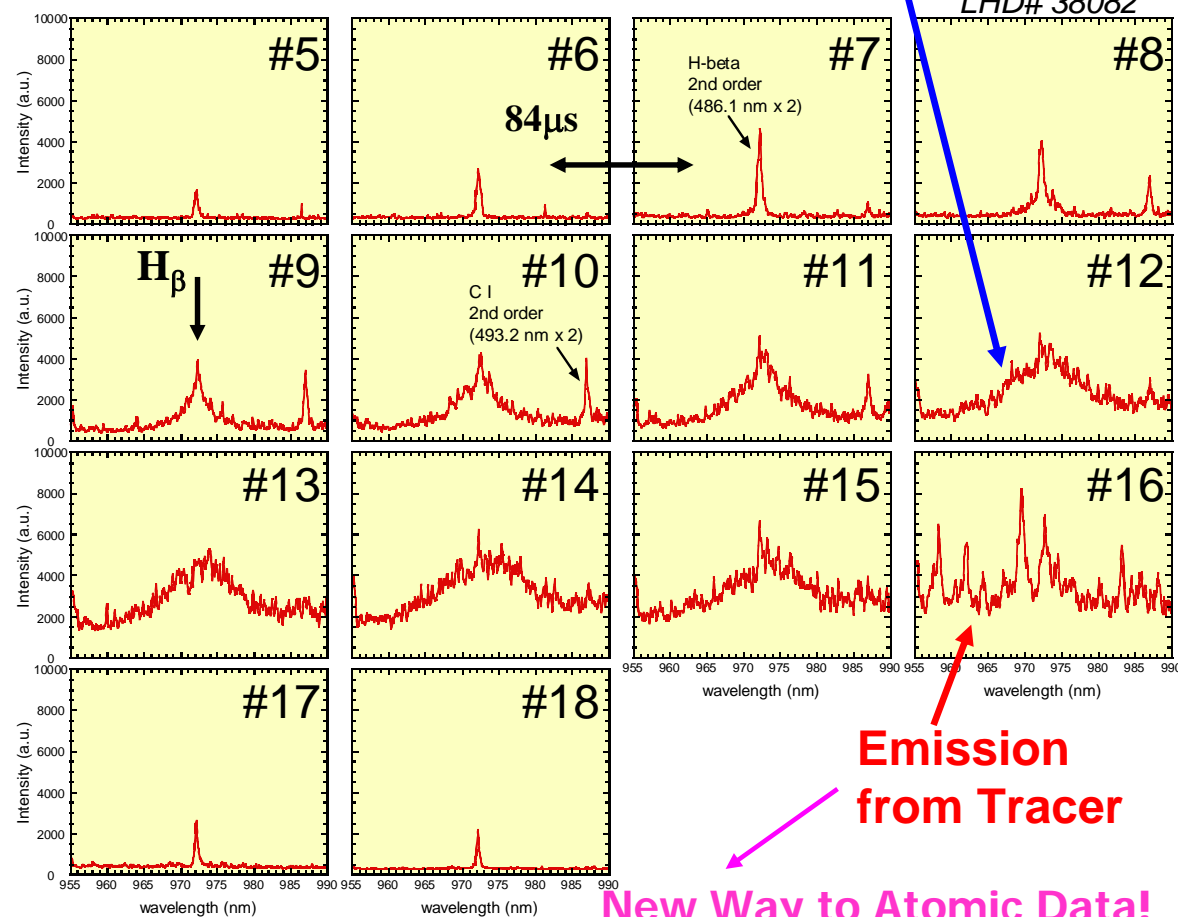
Electron Density in Pellet Cloud!

↑ Stark Broadening of H β

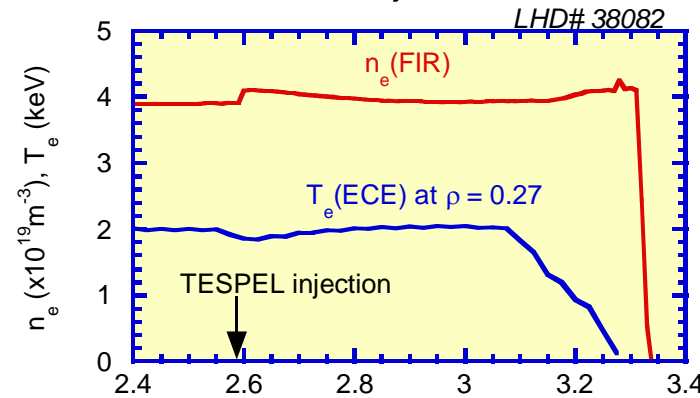
Interference filter + PM

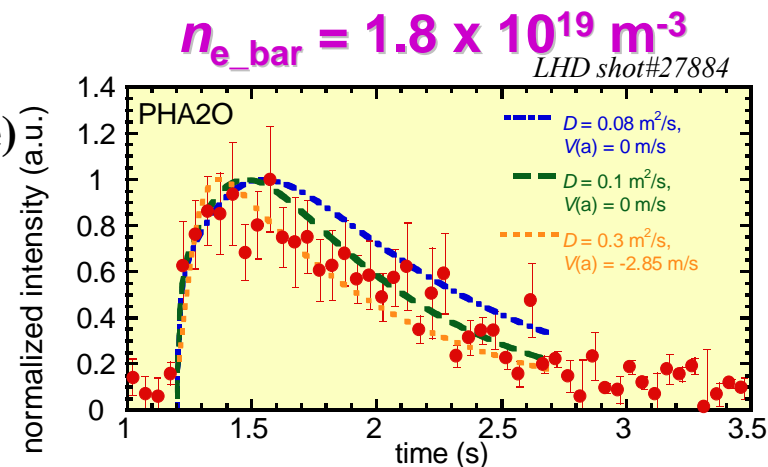
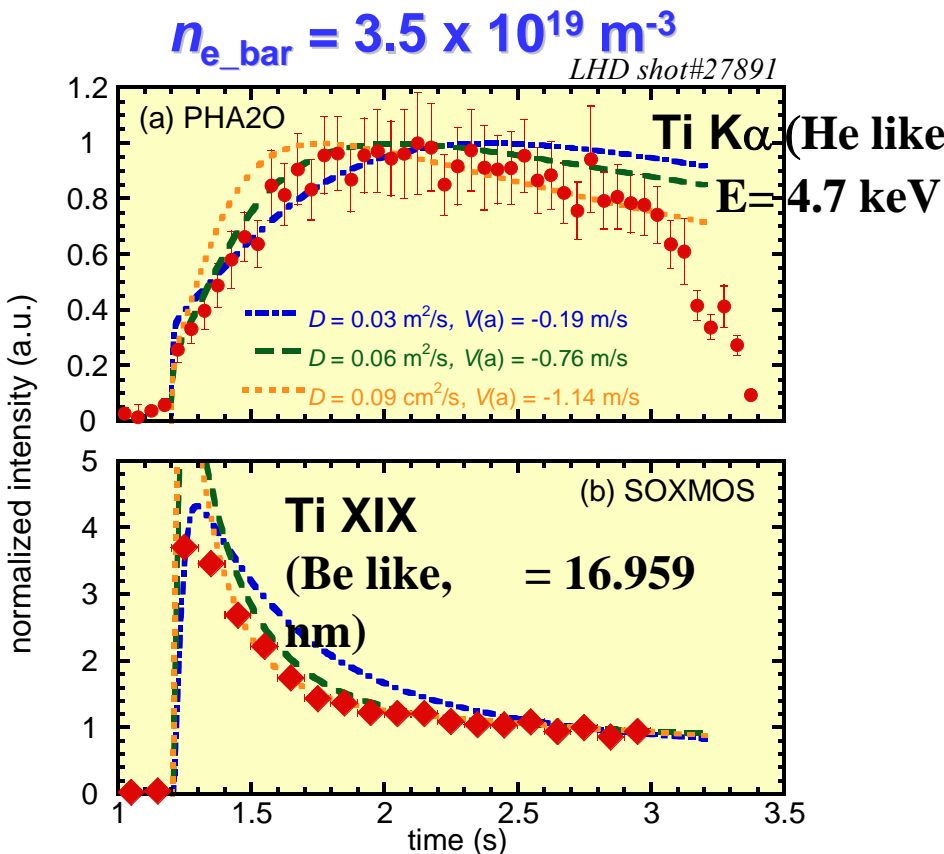


Spectrometer + ICCD Camera



n_e , T_e response to the TESPEL injection





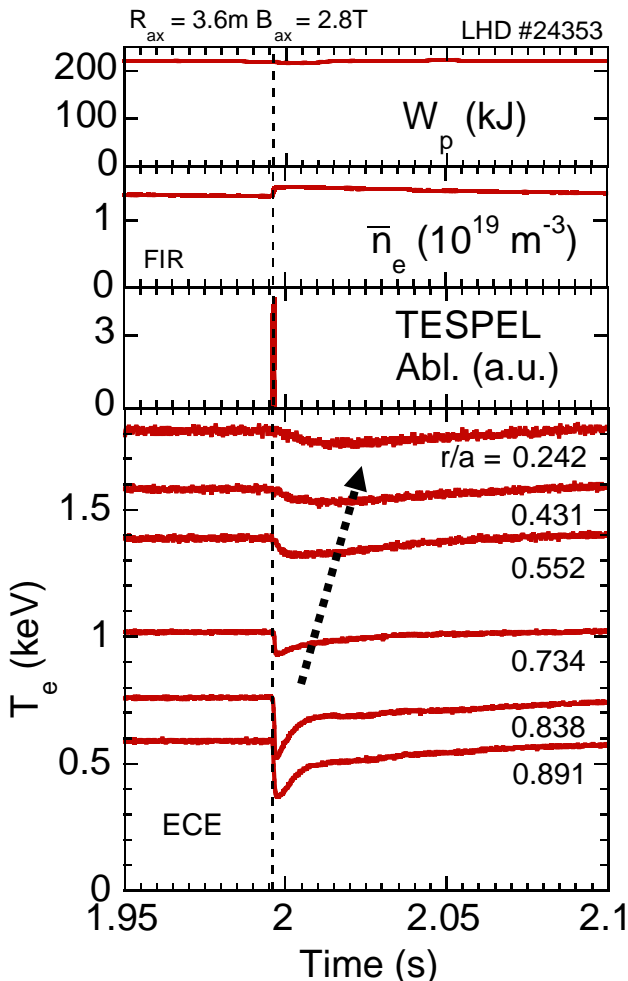
The decay of K α line for the lower density is faster than that of the higher density.

$D = 0.1 \text{ m}^2/\text{s}, V = 0 \text{ m/s}$ fit well with the experimental results for $n_{e_bar} = 1.8 \times 10^{19} \text{ m}^{-3}$.

These temporal behaviors are analyzed with a transport code: MIST. $D=0.06 \text{ m}^2/\text{s}$ and the inward convection velocity of $V(a)= 0.8 \text{ m/s}$ fit well with the data for $n_{e_bar} = 3.5 \times 10^{19} \text{ m}^{-3}$.

Experimental D is larger than the neoclassical ones. This discrepancy is reduced in the higher density case.

Cold Pulse Propagation



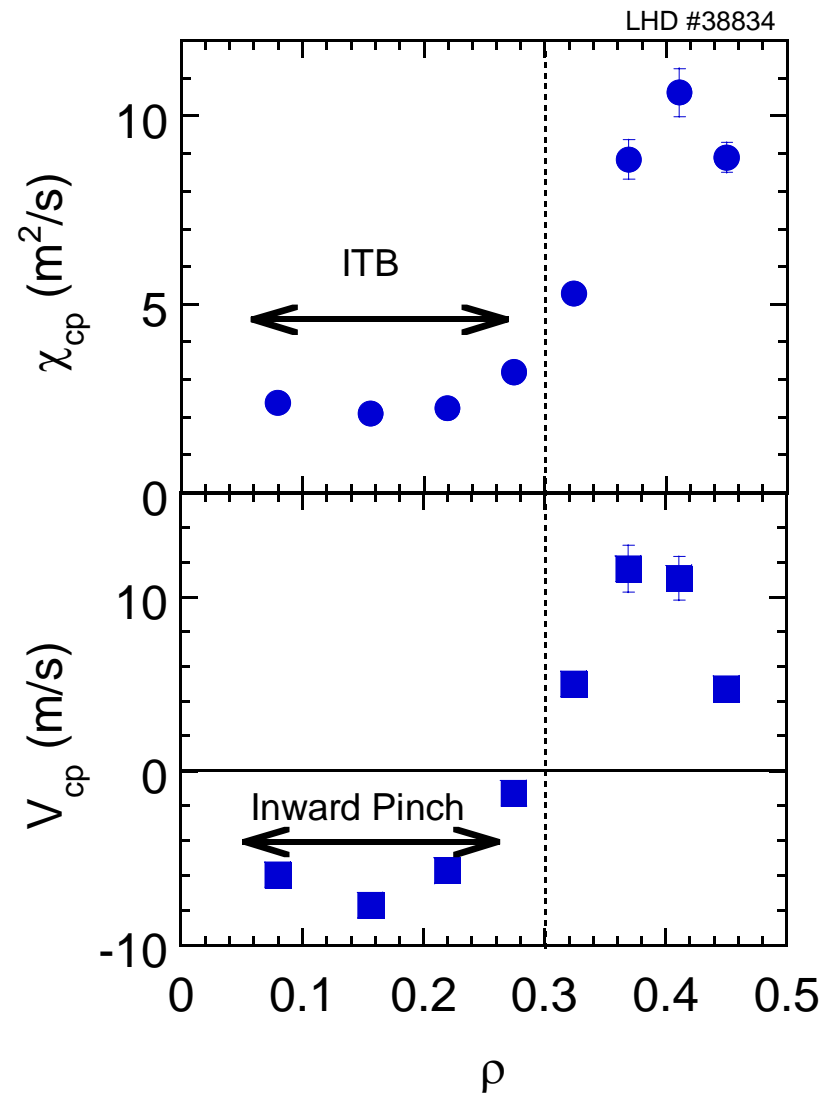
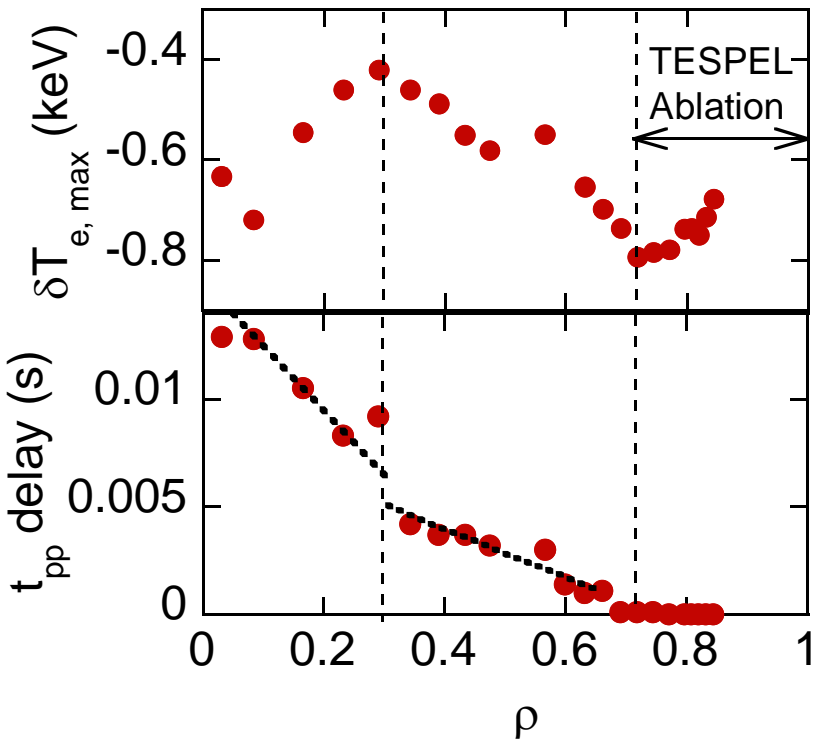
Owing to the flexibility of the size and material, TESPEL injection makes appropriately a sudden drop in the electron temperature in the plasma (~0.5-0.7), the temperature drop (cold pulse) propagates across the flux surfaces. The $T_e(r, t)$ profile is measured every 5 μs with the 32ch radiometer (cross-calibrated with the Michelson interferometer) covering $R_{ax} = 2.9\text{-}3.5\text{ m}$.

● Basic Equations

$$\frac{3}{2} n_e \frac{\partial}{\partial t} \delta T_e = \nabla \cdot \left(n_e \chi_{tr} \nabla \delta T_e - \frac{3}{2} n_e V_{tr} \delta T_e \right)$$

The transport equation for the perturbation is solved numerically and compared with the experimental data to obtain heat conduction coefficient χ_{tr} .

- TESPEL cold pulse technique is used to analyze the heat transport in the ITB region.
- Transport changes significantly at the barrier (~ 0.3).
- Reduced χ and Heat pinch are observed.

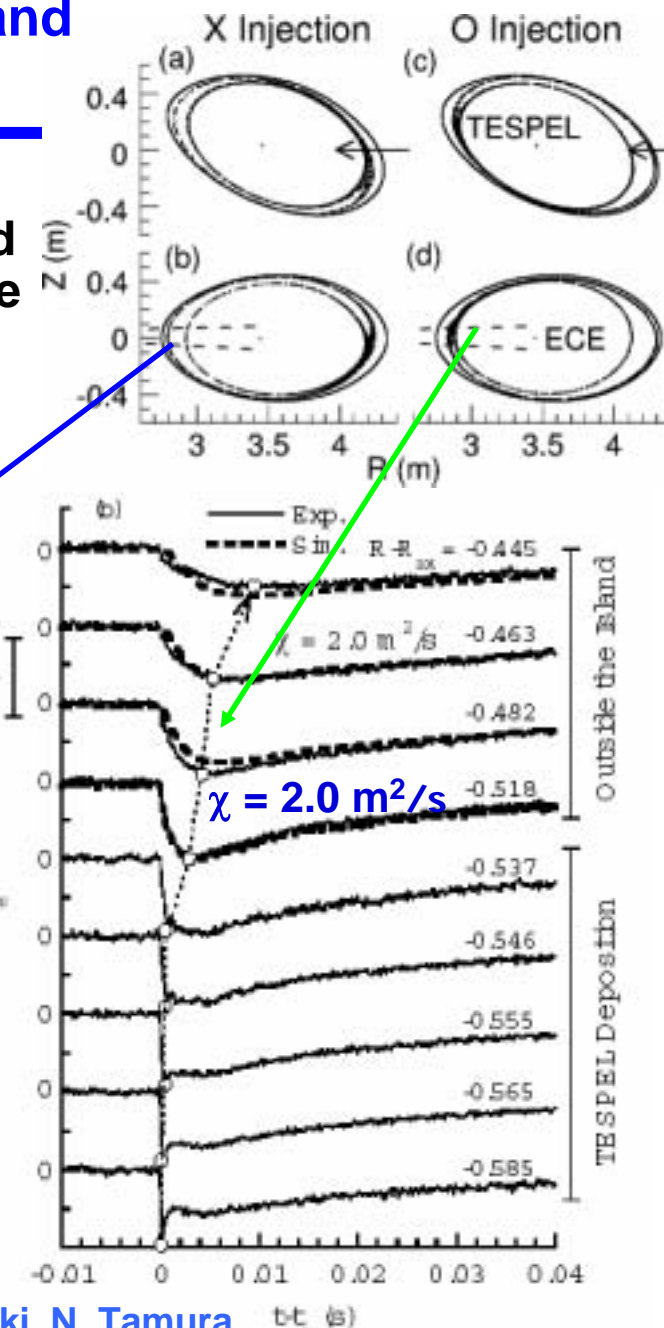
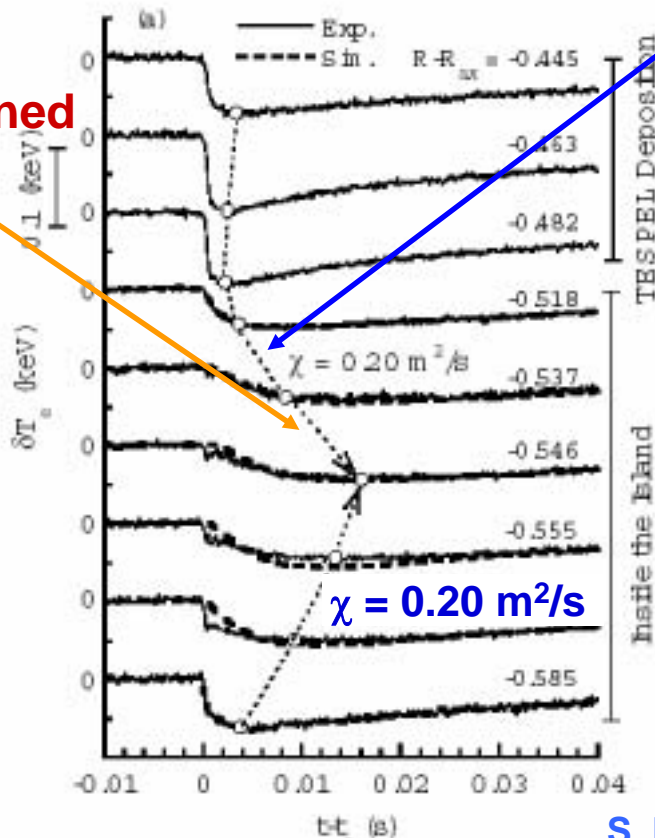


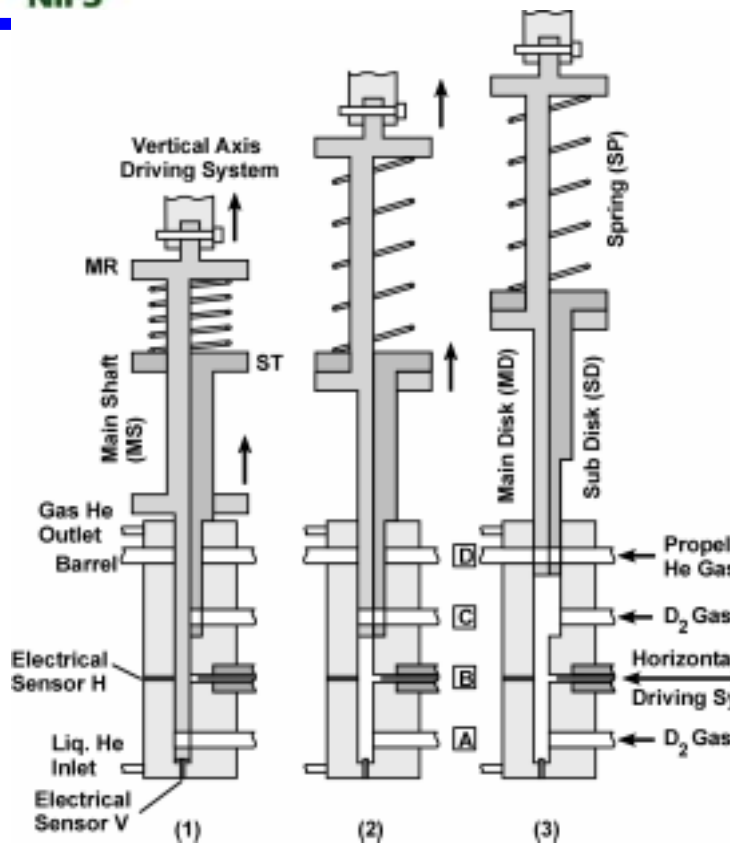
Cold pulse propagation in magnetic island induced by TESPEL

- When TESPEL is injected at X-point, not much direct interference in the magnetic island. The cold pulse in the core region propagates fast, but inside of the magnetic island the cold pulse propagates very slowly. Thus, the low heat conductivity of $\chi_e = 0.2 \text{ m}^2/\text{s}$ was obtained, while $\chi_e = 2 \text{ m}^2/\text{s}$ in the core plasma.

Reduced χ is obtained Inside the Island

- R is the major radius and the last closed magnetic surface is at $R - R_{ax} = -0.7 \text{ m}$.
- The ECE receiving antenna is mounted in the inboard side of LHD.



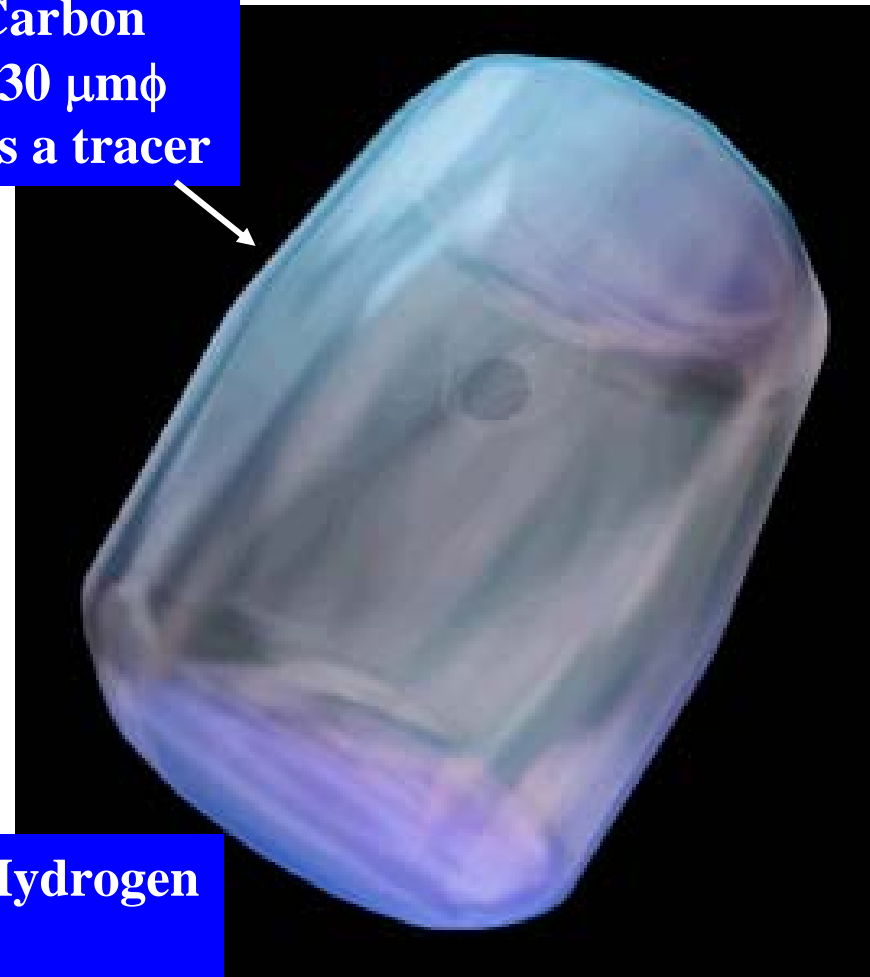


TECPYL-1

Patents: S. Sudo (1996) in:
Japanese Patent No. 2113888
USA Patent No. 54887094
EPC Patent No. 647087

S. Sudo: "Diagnostics on LHD", EPS2003, St. Petersburg, 7-11/2003.

Carbon
230 $\mu\text{m}\phi$
as a tracer



Solid Hydrogen
3 mm ϕ

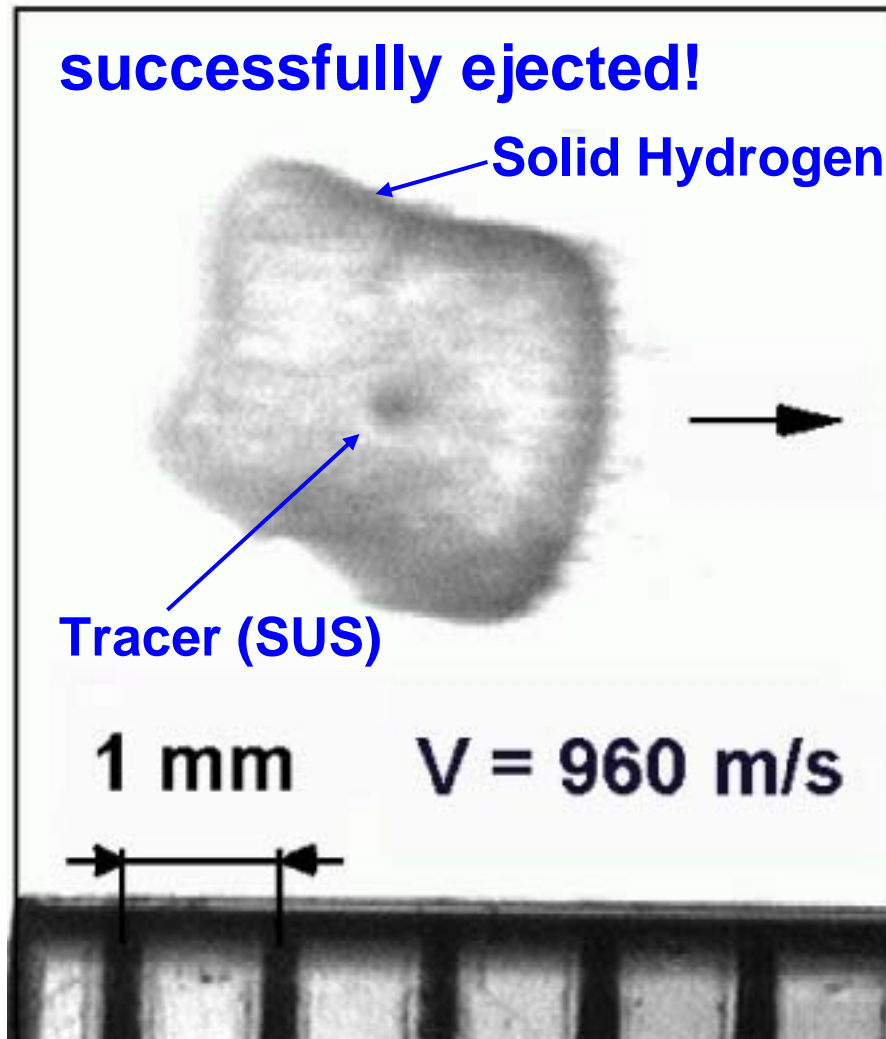
S. Sudo, "Tracer-encapsulated cryogenic pellet production for particle transport diagnostics,"
Review of Scientific Instruments, Vol. 68 No. 7 (1997).



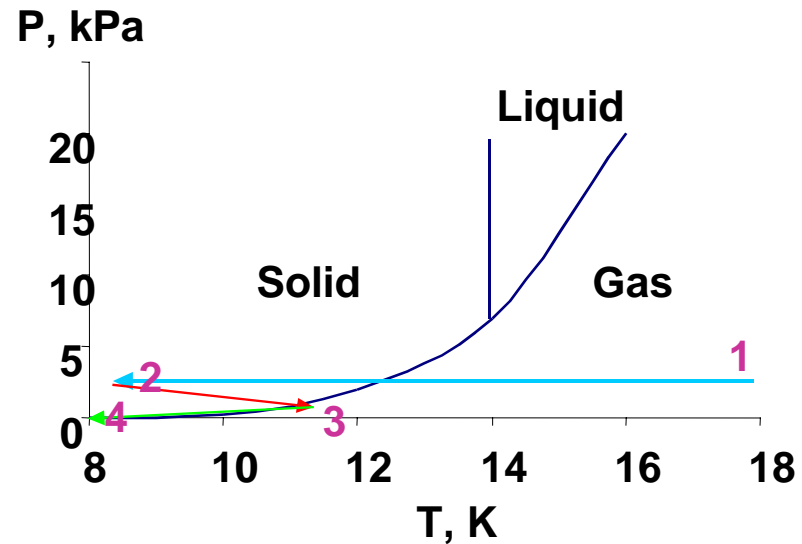
T= 8K Solid H₂

SUS Ball 200μmφ

TECPEL in Flight



With gas gun utilizing high pressure helium gas (~30 atm.), TECPEL is ejected, and the photo of TECPEL in flight is taken. This shows also the remaining Tracer.



Summary

- ◆ Standard diagnostics for fundamental plasma parameters (T_i , T_e , n_e) and for plasma physics are routinely utilized for daily operation and physics studies in LHD with high reliability and flexibility.
- ◆ Diagnostics for steady state plasma are developed including a data acquisition system for handling large amount of data.
- ◆ 2-D or 3-D diagnostics are intensively developed:
 - ❖ Tomography (Tangential SX CCD, Bolometer)
 - ❖ Imaging (Bolometer, ECE, Reflectometer)
- ◆ Diagnostics for edge physics, needed for steady state operation, are developed and installed in LHD.
- ◆ Advanced diagnostics are also being developed in LHD through domestic and international collaborations.

New proposals for collaboration at LHD are welcome!